Characterization and Design of Nanomaterials Through Multiscale Modeling & Simulation

Tahir ÇAĞIN

Laboratory for Computational
Engineering of Nanomaterials and Devices

http://che.tamu.edu/orgs/groups/Cagin/

Artie McFerrin Department of Chemical Engineering

Texas A&M University

E-mail : cagin@che.tamu.edu

Summary

- Rational Design and Characterization via Modeling and Simulation
- Multiscale Modeling Hierarchy and Materials Simulation
- Examples of Applications in Functional Materials
  - Multiscale modeling PMMA Thin Films
  - Hydrogen storage and Delivery (MOFs)
  - Thermo-electrics
  - Piezo-electrics and Ferro-electrics
  - Amplified Flourosence Quenching Polymers for IED sensing
  - Structure, Assembly and Transport in Cyclic Peptide nanotubes (CPNT)
  - Stress Corrosion Cracking in Fe based alloys
  - Nuclear Fuel materials
  - Damage Cascade Simulations
  - Magnetic Shape Memory Alloys

Design/Characterization Through Modeling Paradigm

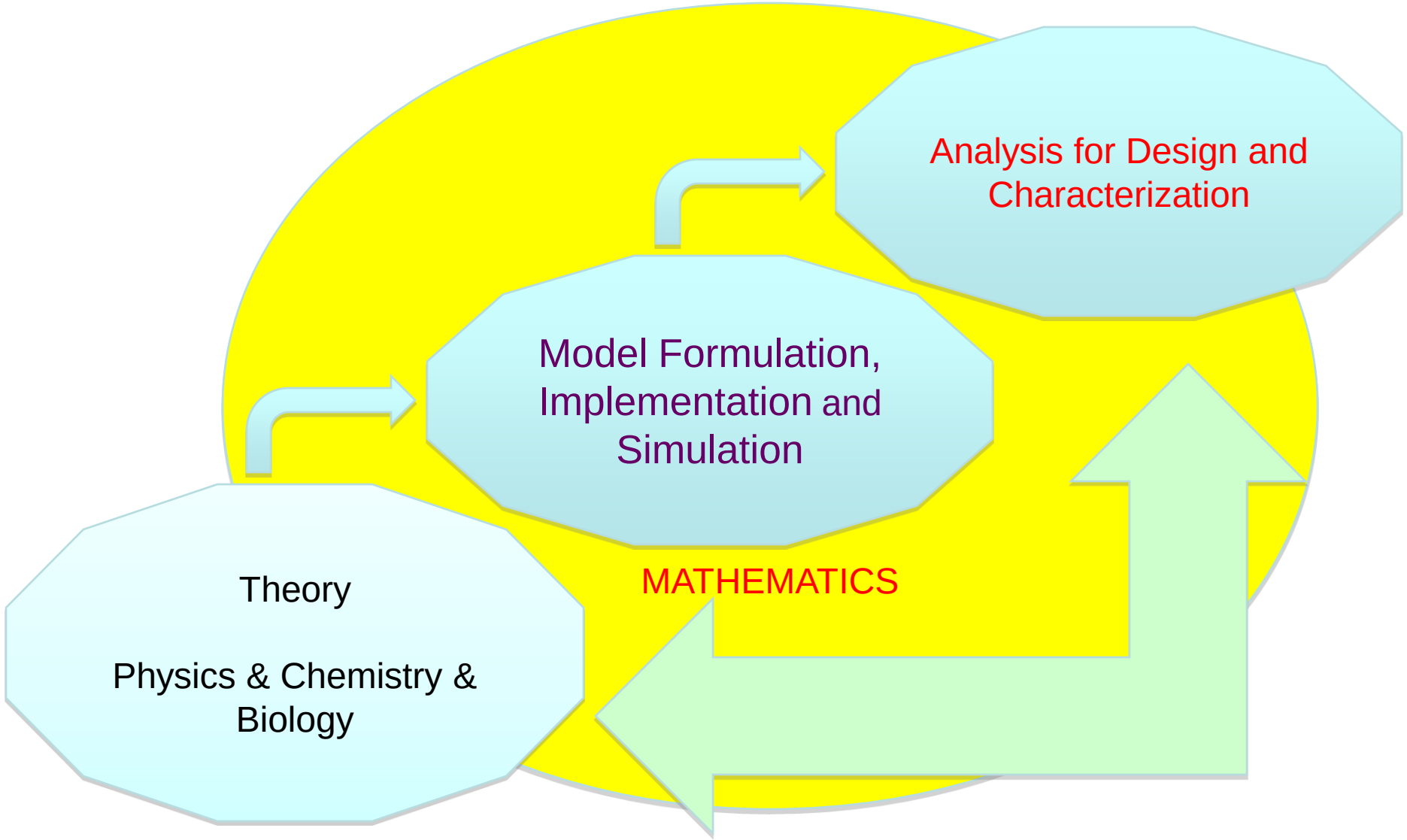

Multiscale Simulation and Modeling Hierarchy

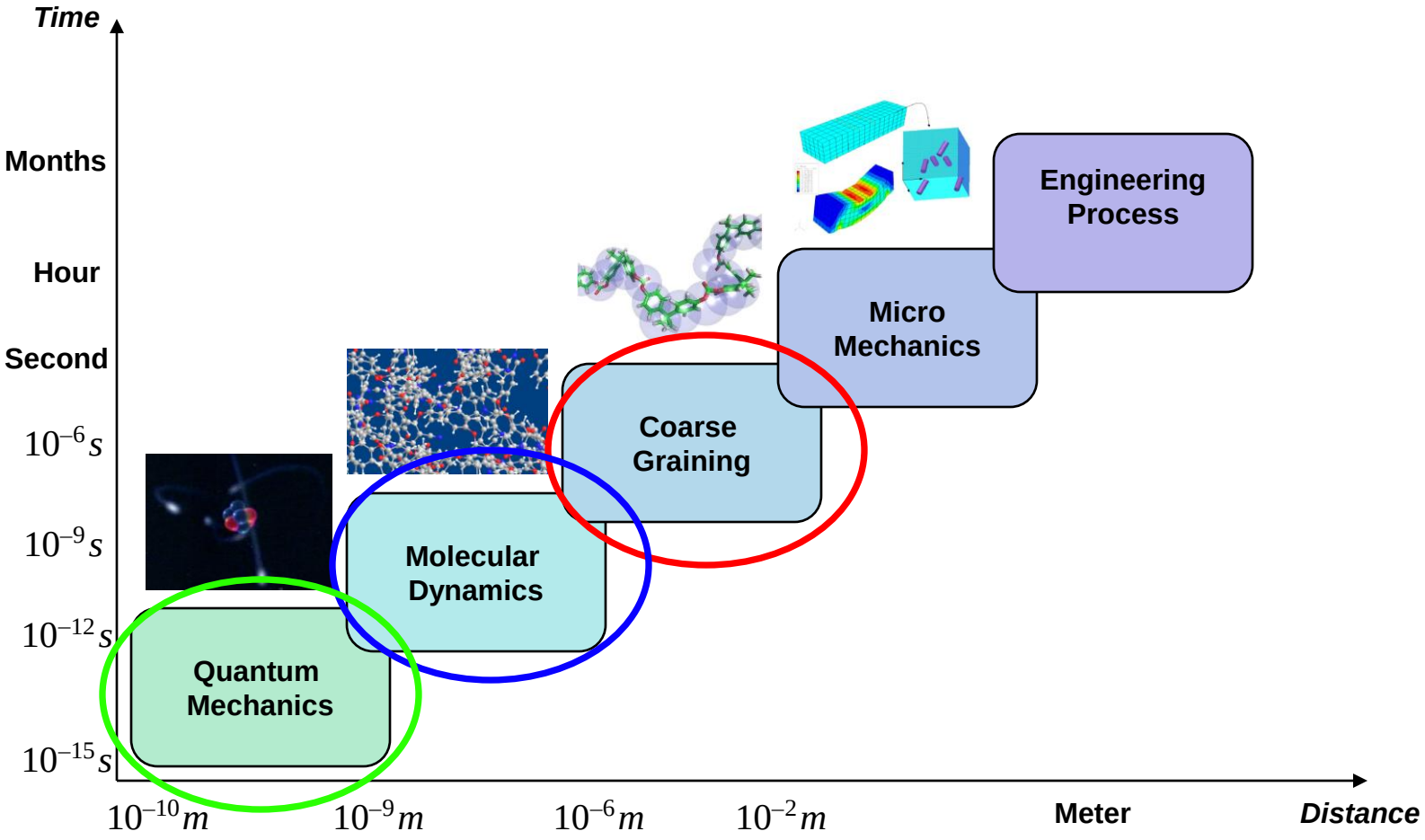

Multiscale modeling of PMMA Thin Films for Microelectronics Applications

Develop a methodology for the numerical simulation of large models of polymeric thin films so that realistic estimation of mechanical and thermal properties can be obtained.

Diffusive equations, like the Fourier eq. for conduction heat transfer, do not account for the effect of energy carriers (i.e. phonons) in thermal properties.

Molecular Dynamic simulations can be implemented to solve this problem.

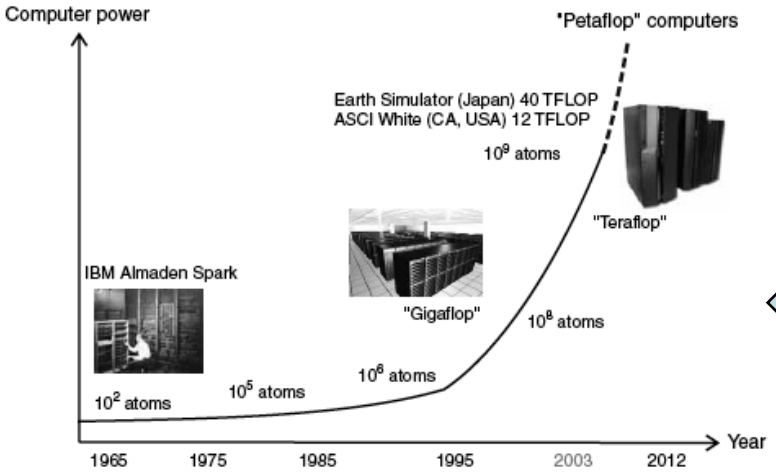

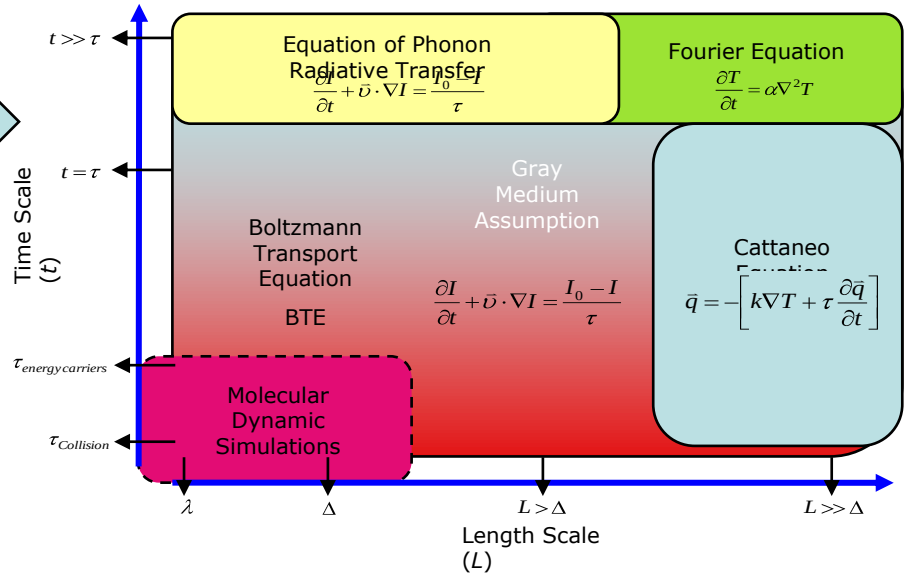

However, the computer resources needed to simulate a film of the necessary length and time scale (few tens of nanometers, microseconds) are prohibitive.

Coarse Grain Molecular Dynamics

- Groups of atoms represented by a single bead
- Used for complex molecules in biosciences (proteins, DNA)
- Used in simulations of entangled polymer melts

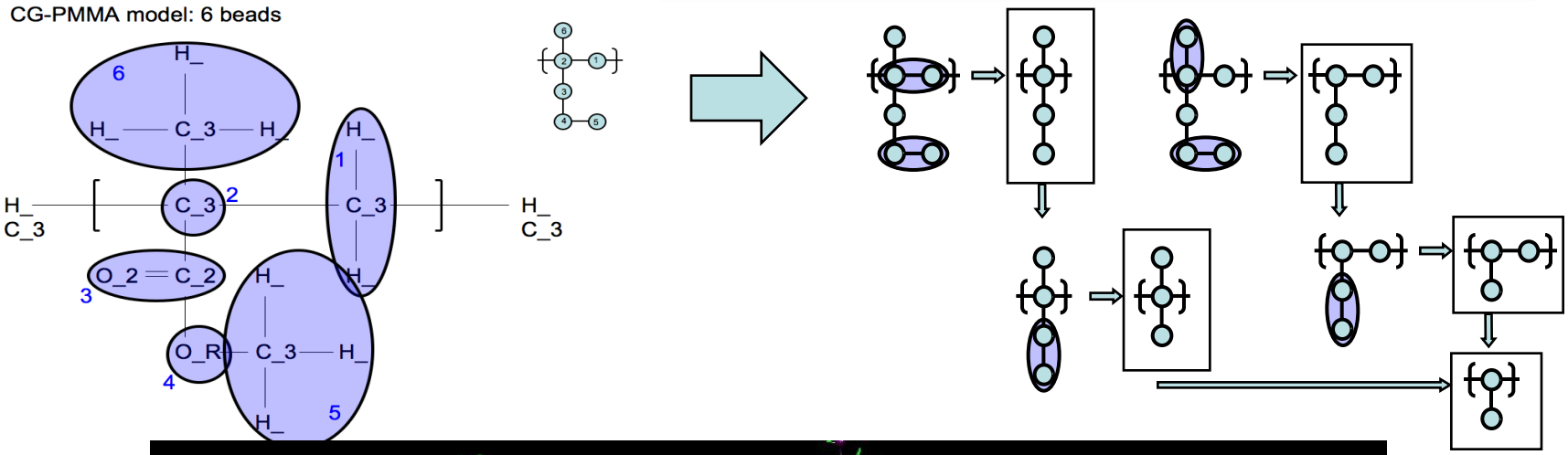

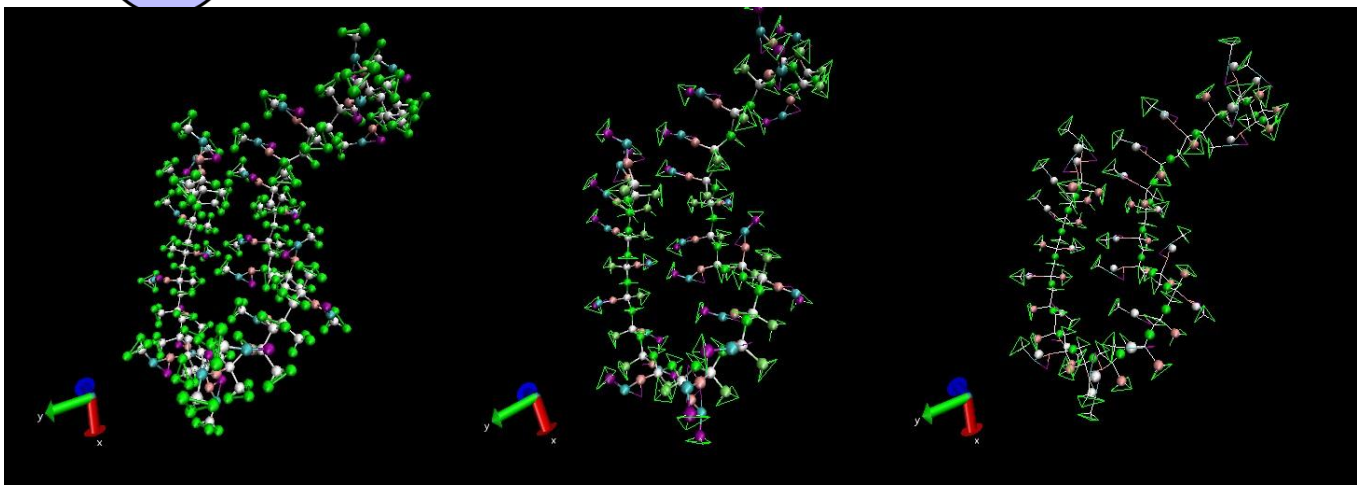

Benefits

	1 ns, local comp. (4-proc)		100 ns, Hydra (16-proc)	
Model	Atoms/Beads	Run time (hrs)	Atoms/Beads	Run time (hrs)
Atomistic	2256	25.58	18002	~ 1000
6 Beads	900	4.85	7200	165.0
4 Beads a	600	2.05	4800	46.6
4 Beads b	600	2.45	X	
3 Beads a	450	1.28	3600	21.1
3 Beads b	450	1.90	X	
2 Beads	300	0.85	X	

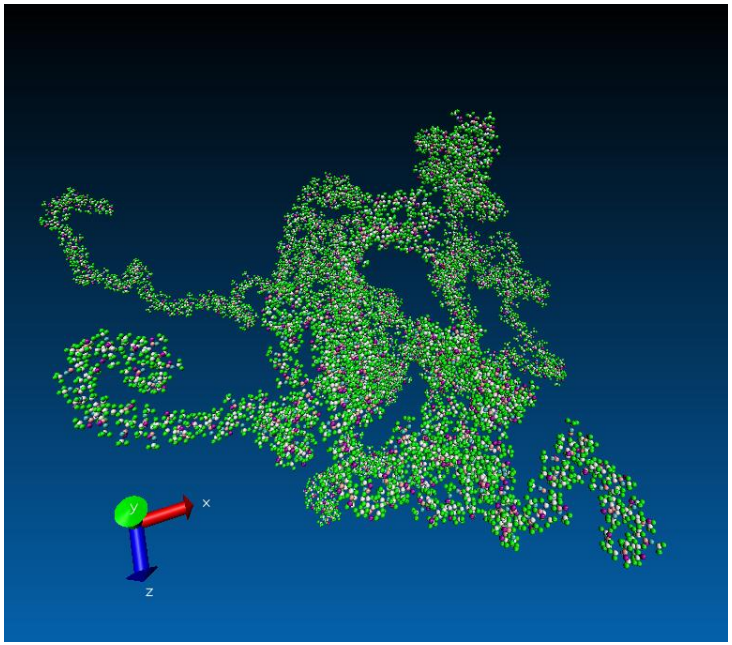

A system of 18k atoms of PMMA is a 5x5x5 nm box.

Few tens of nanometers and microseconds are now attainable

A 20x5x5 nm box of 3-bead model running for 1 μs on Hydra (64-proc) will take ~ 14 days.

Metal Organic Framework (MOF) for High Capacity Hydrogen Storage and Delivery

M. Mani Biswas, T. Cagin

- Crystalline material
  - Metal oxide clusters at vertexes,
  - Connected by organic linkers.
- Porous, large surface area (2500 - 5000 m^2/gm)
- Low density (0.59 gm/cc)

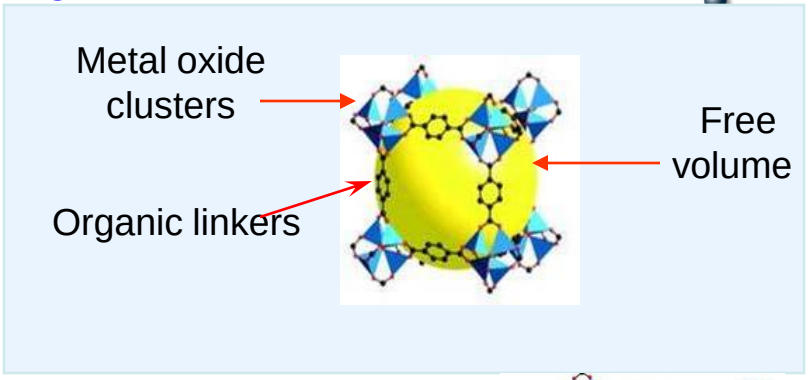

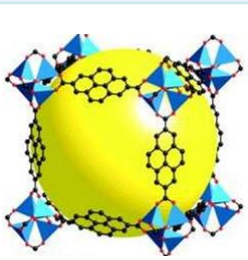

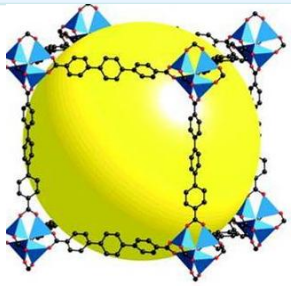

- Crystals can be designed
  - Geometry, pore size can be varied (3.8 - 30 Å)
  - Linker molecule of different chemistry can be chosen

- Selective storage of guest molecule inside free volume
  - Hydrogen gas storage, gas separation
  - Drug delivery vehicle
- Designable property
  - Catalysis, molecular detection

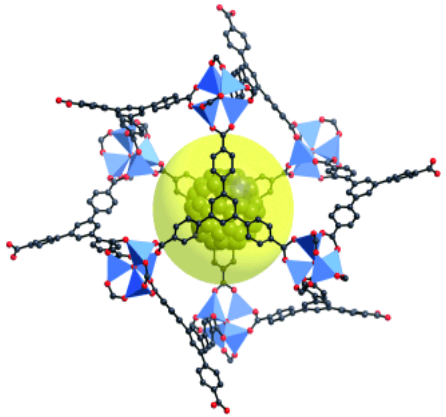

Ref: Li, H.; Eddaoudi, M.; O.Keeffe, M.; Yaghi, O. M., (1999) Design and synthesis of an exceptionally stable and highly porous metal-organic framework, *Nature*, 402, p. 276.

Theoretical Investigation using Classical MD simulations and Quantum Level calculation
- properties of Metal Organic Frameworks (MOF) for efficient hydrogen storage and delivery

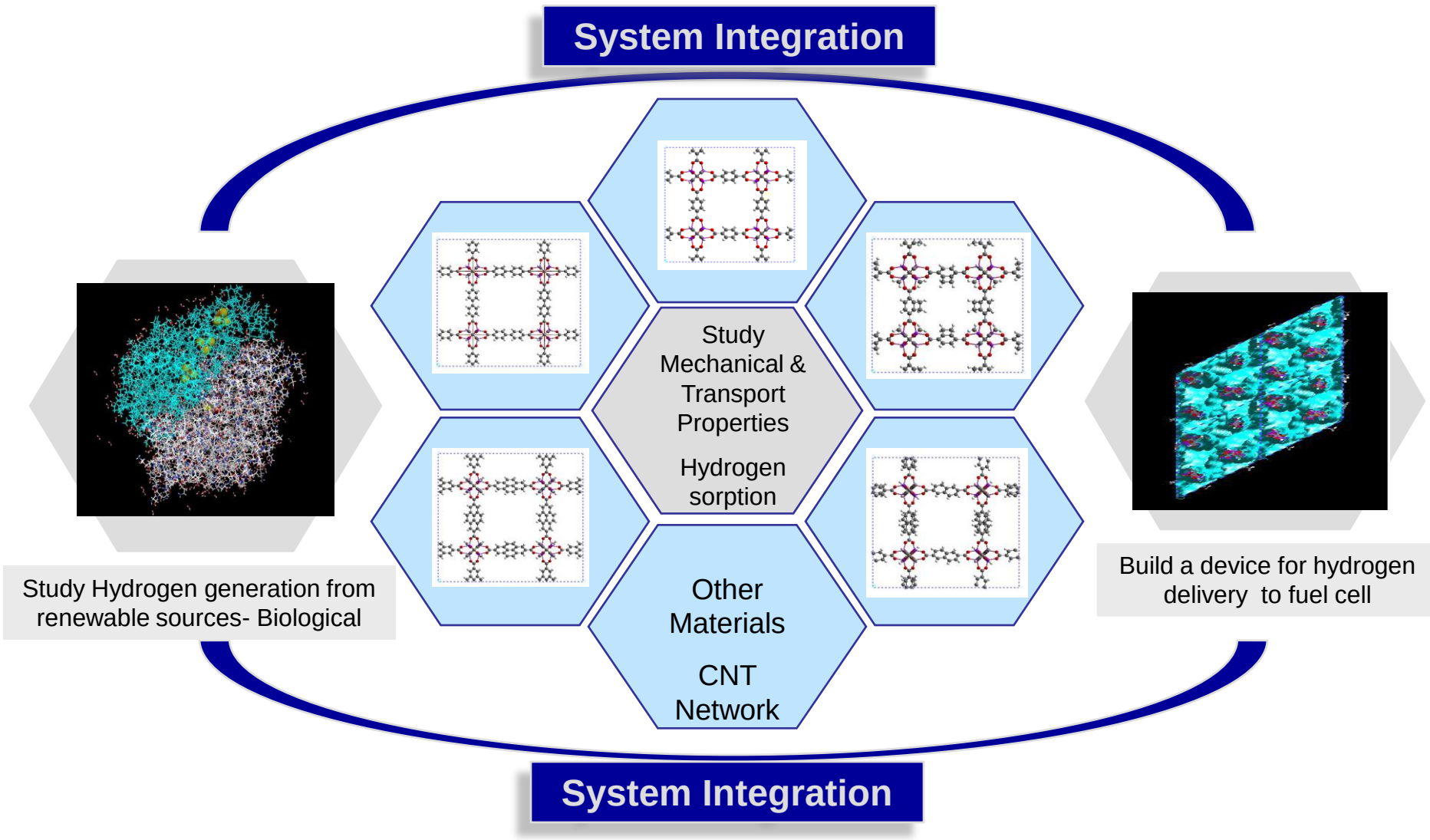

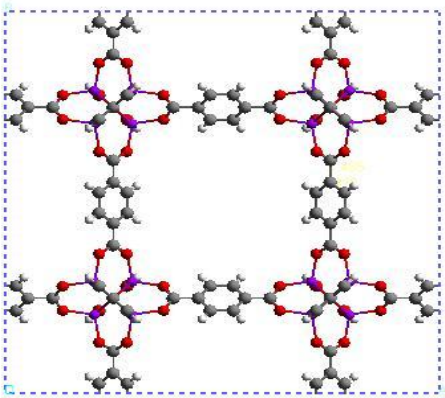

Loading at 100 MPa (298k)

Depressurize at 100 MPa

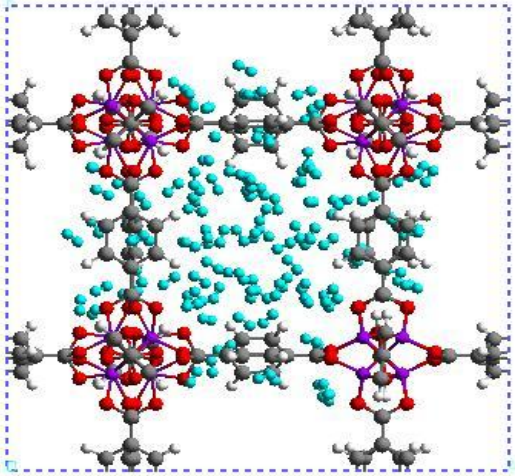

Unloading at 300 MPa (298k)

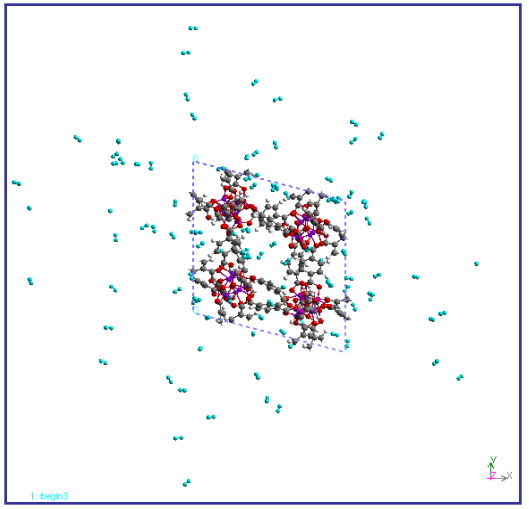

M. Mani-Biswas, T. Cagin, “Shape memory effect in MOFs”, to be submitted.

Ferroelectrics & Piezoelectrics

Domain Wall: Interface of polarization domains

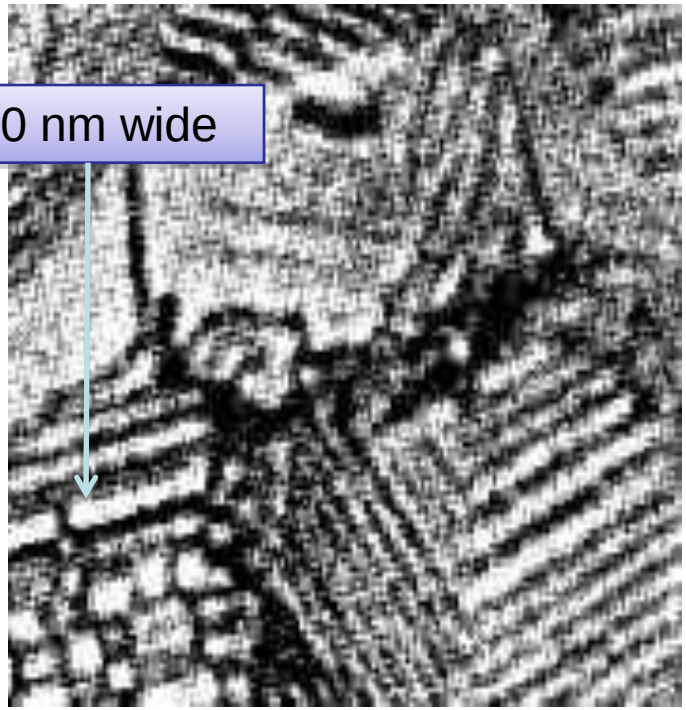

http://www.materials.leeds.ac.uk/luec/ActMats/Domain2.jpg

- Determine piezoelectric response and macroscopic polarization
- Fatigue switchable polarization
- Used in many applications
  - RAM
  - Actuators
  - Transducers
  - Sensors

Zhang, Cagin, Goddard, PNAS 103, 14695 (2006); Cagin et al, CMES 24, 215 (2008); Majdoub, Sharma, Cagin, PRB 78, 12407 (2008); PRB 77, 125424 (2008)
J. Haskins, A. Kinaci,T. Cagin in progress.

Simulations excel in investigating nanostructures and the origin of bulk properties.

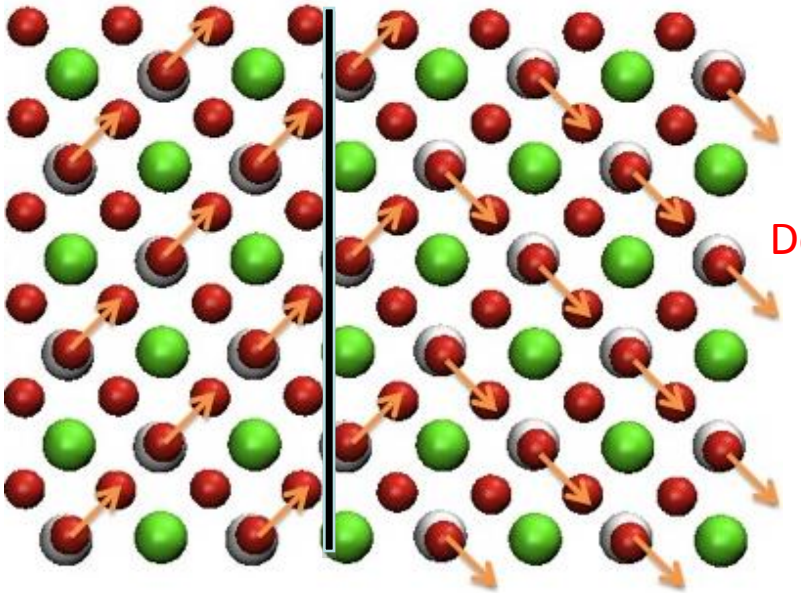

Domain Walls

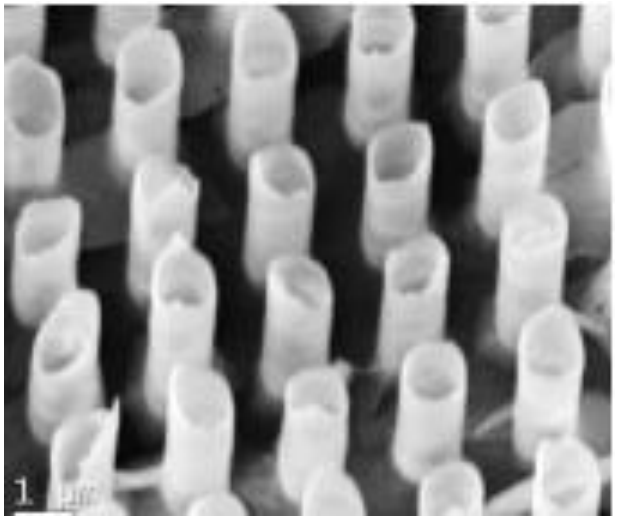

PZT nanotubes for memory devices

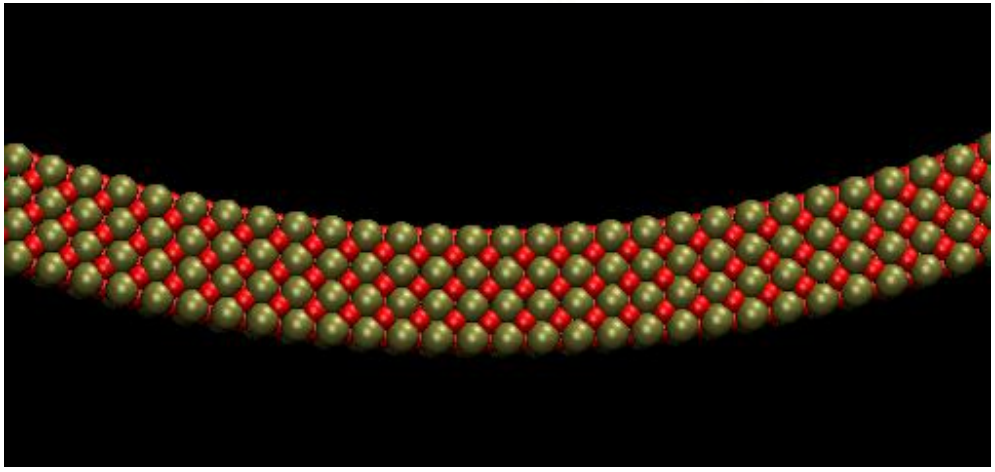

Nonlinearly strained cantilever polarization enhancement

Temperature behavior of PZT calculated by polarizable force fields.

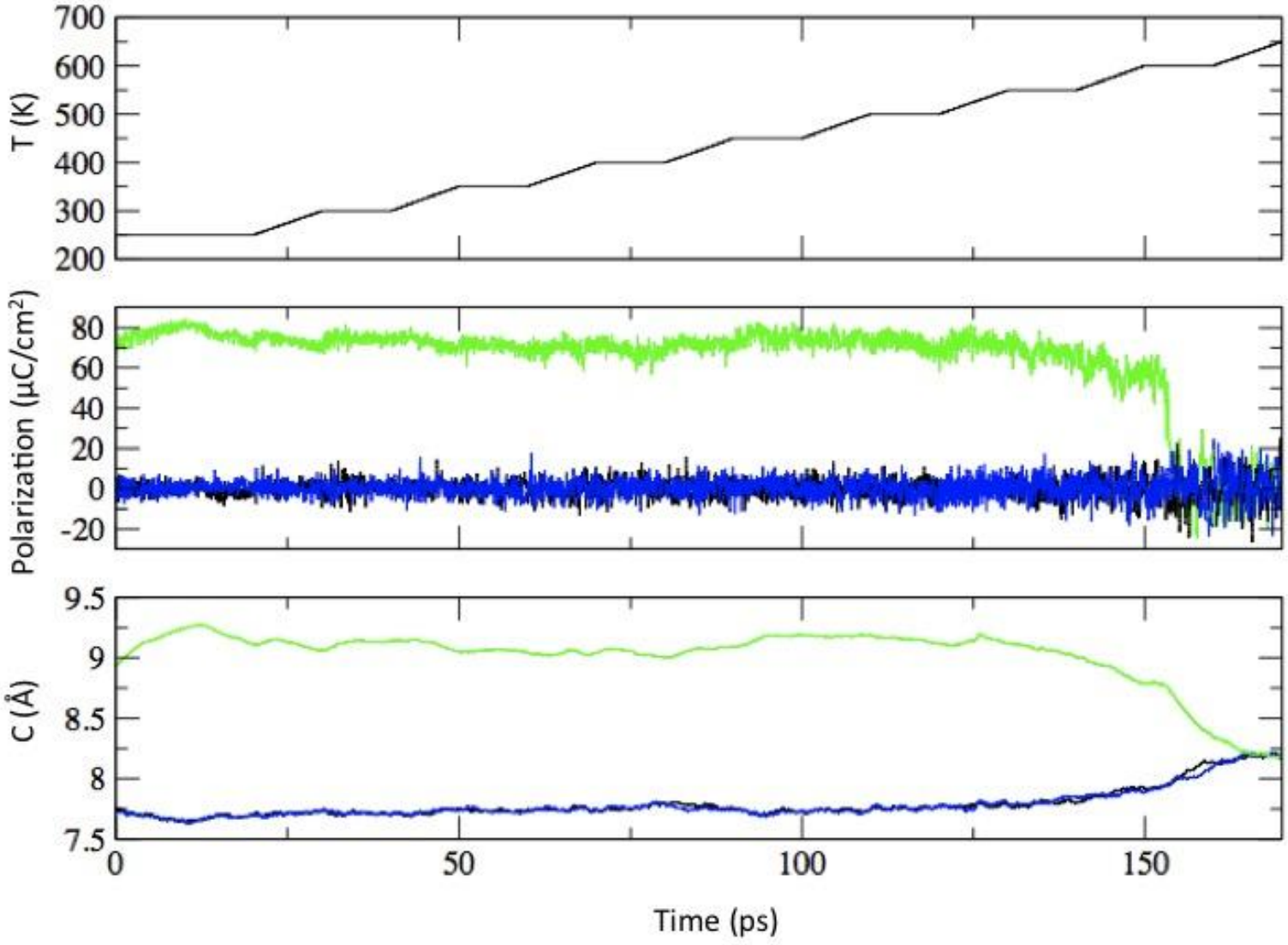

Hysteresis behavior of PT and PZT.

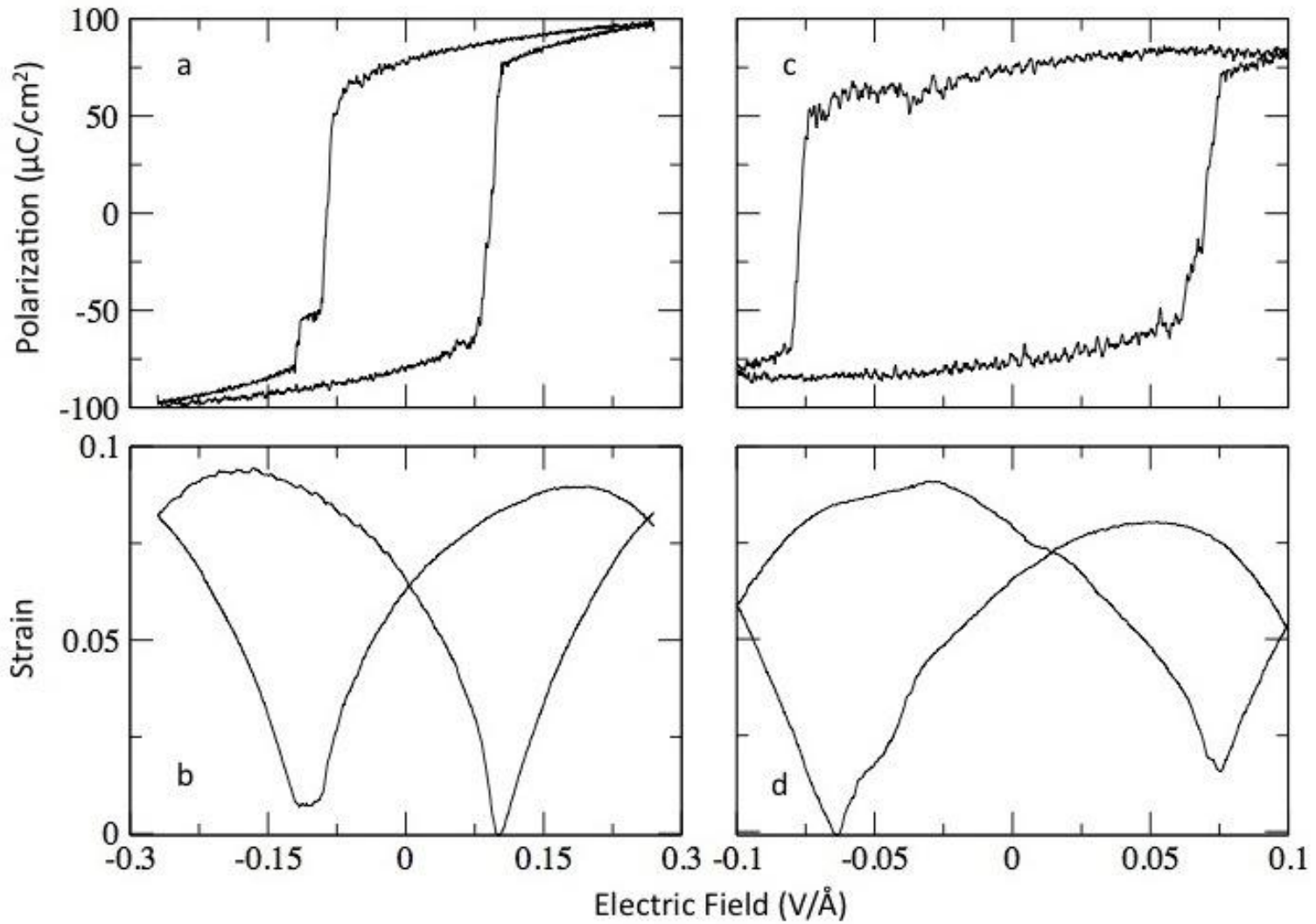

Triangle field of 1 GHz with maximum strength of 0.27 V/Å .

The simulations shows characteristic ferroelectric hysteresis behavior.

ThermoElectrics, Performance Criteria: *Figure of Merit*

Problem : Inter-dependence of σ, κ and S through carrier concentration.

$$ZT = \frac{S^2 \sigma}{\kappa} T$$

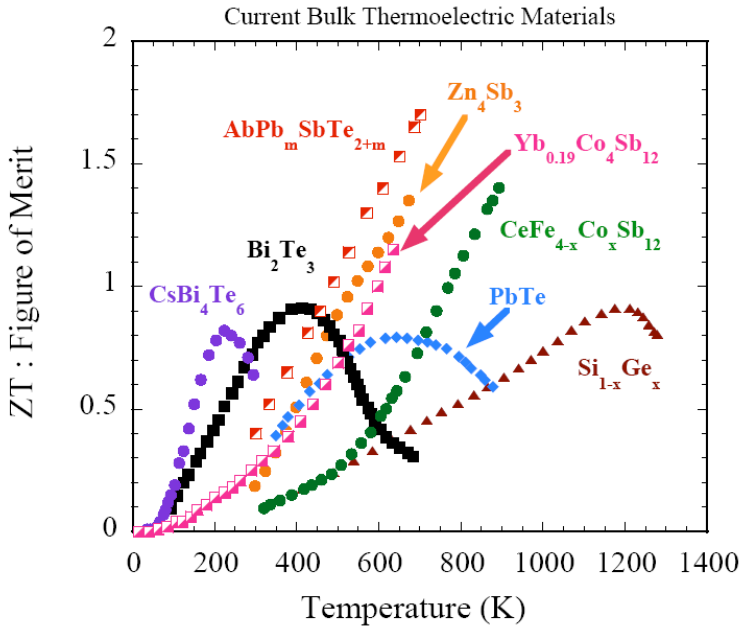

Increasing ZT is difficult - conflicting Properties

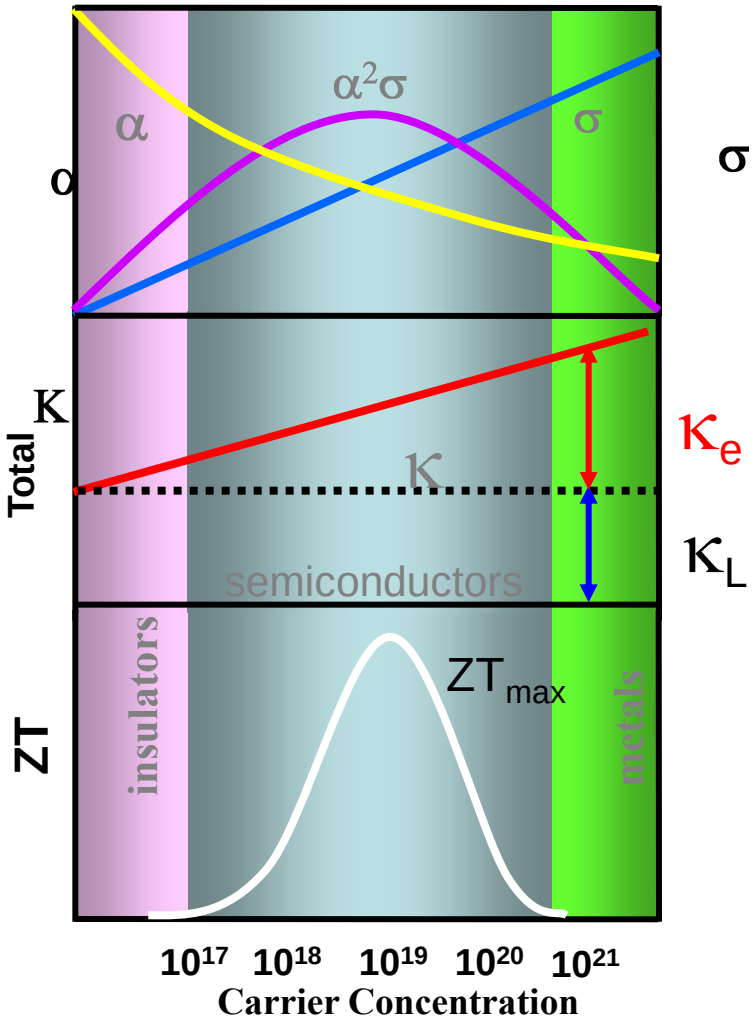

GF Wang and T. Cagin, Appl. Phys. Lett. 89, (2006) 152101

GF Wang and T. Cagin, Phys. Rev. B 75 (2007) 075201

C. Sevik, T. Cagin, in progress

A. Kinaci, C. Sevik, T. Cagin, in progress

Transport Properties From Ab initio Theory

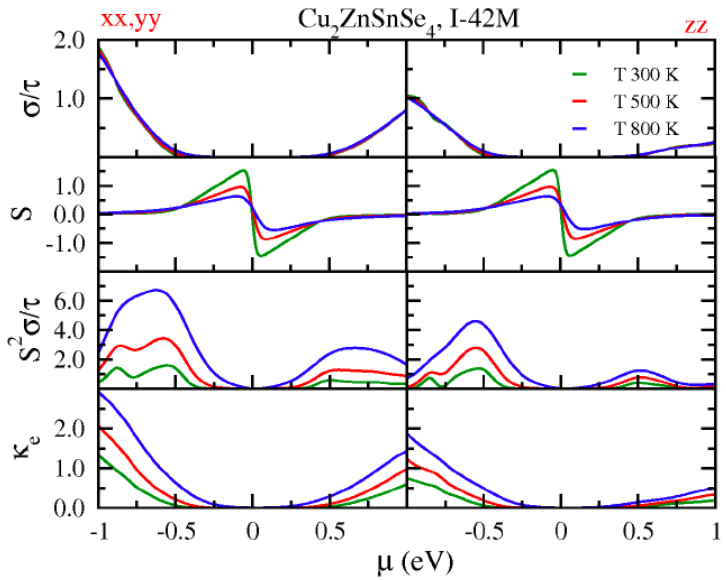

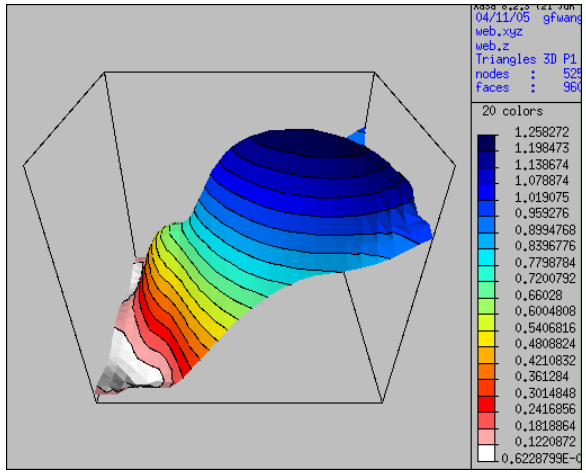

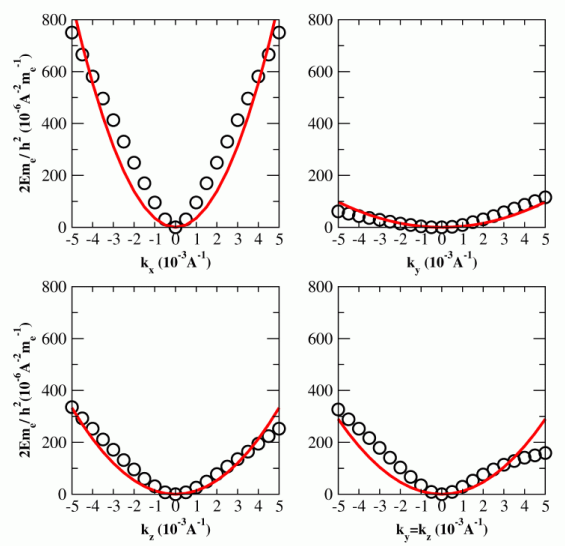

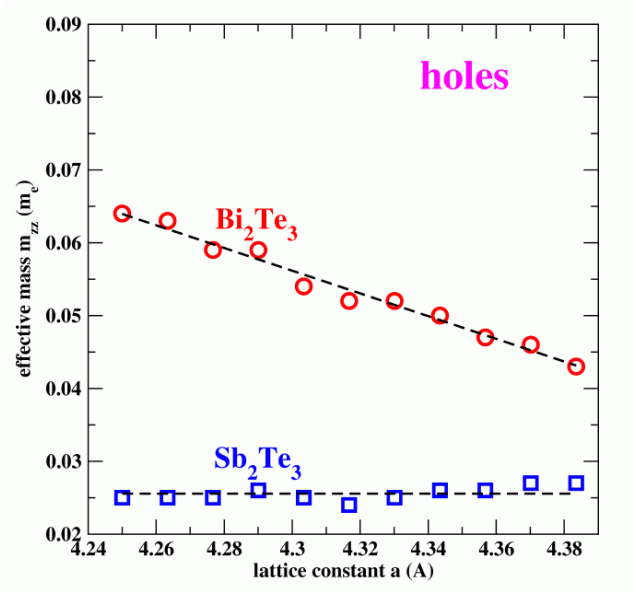

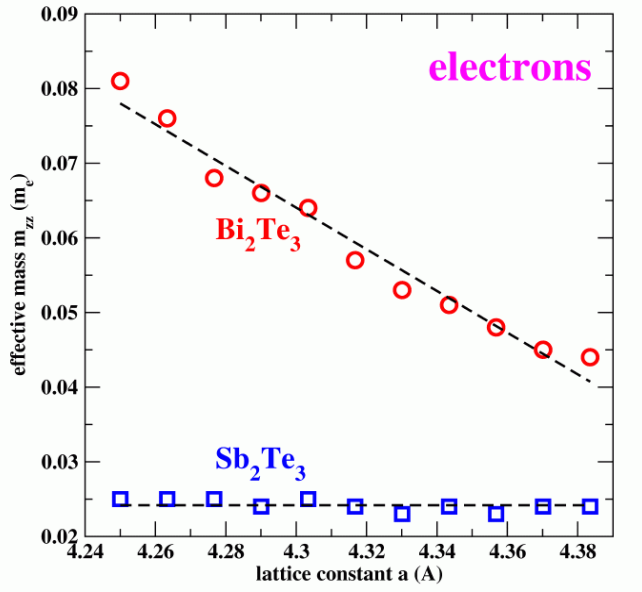

New trends in thermoelectrics: Complex oxides and structural miniaturization (superlattices, nanowire, quantumdots …)

Manipulating properties of $SrTiO_3$

- External stress
- Chemical alloying
- Controlled defects
- Structuring in atomic scale etc…

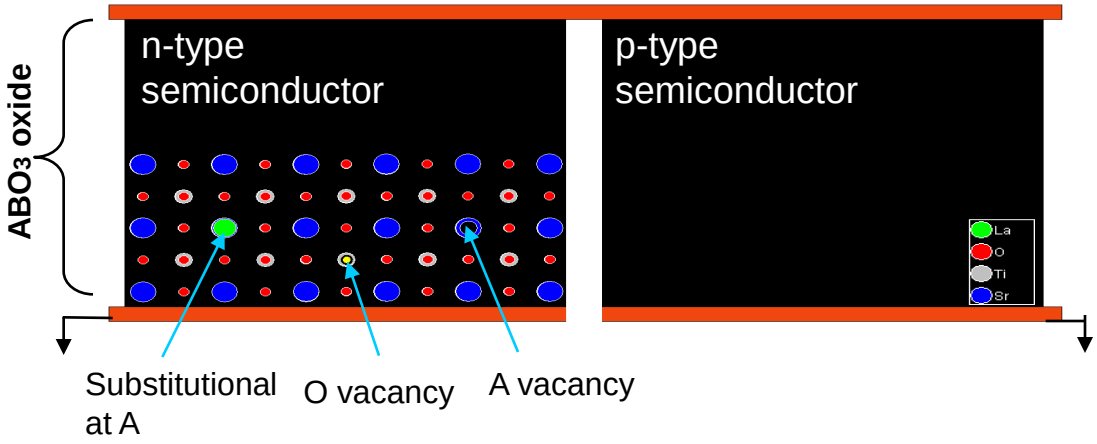

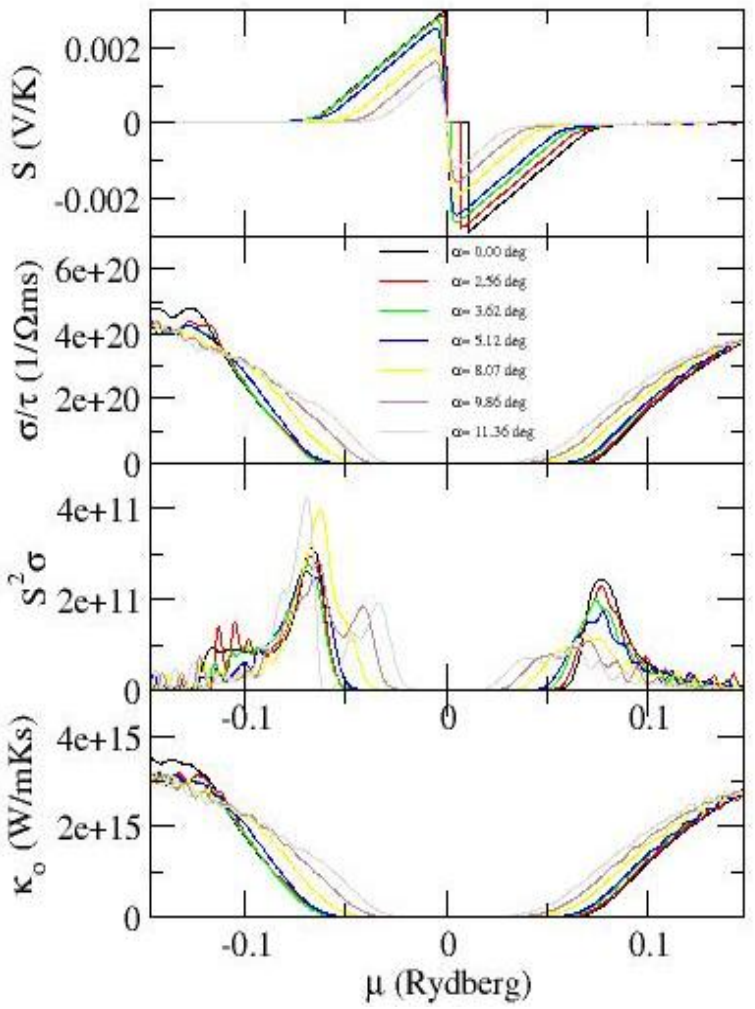

Effect of simple shear on conduction properties of $SrTiO_3$

Structure and Chemistry at interface of Si-nc & silica

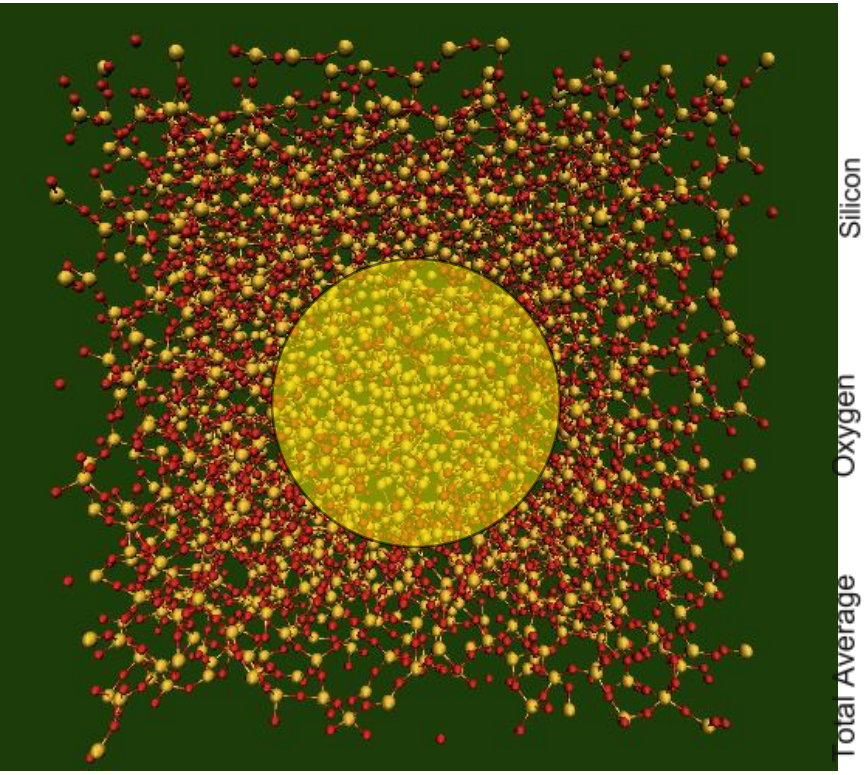

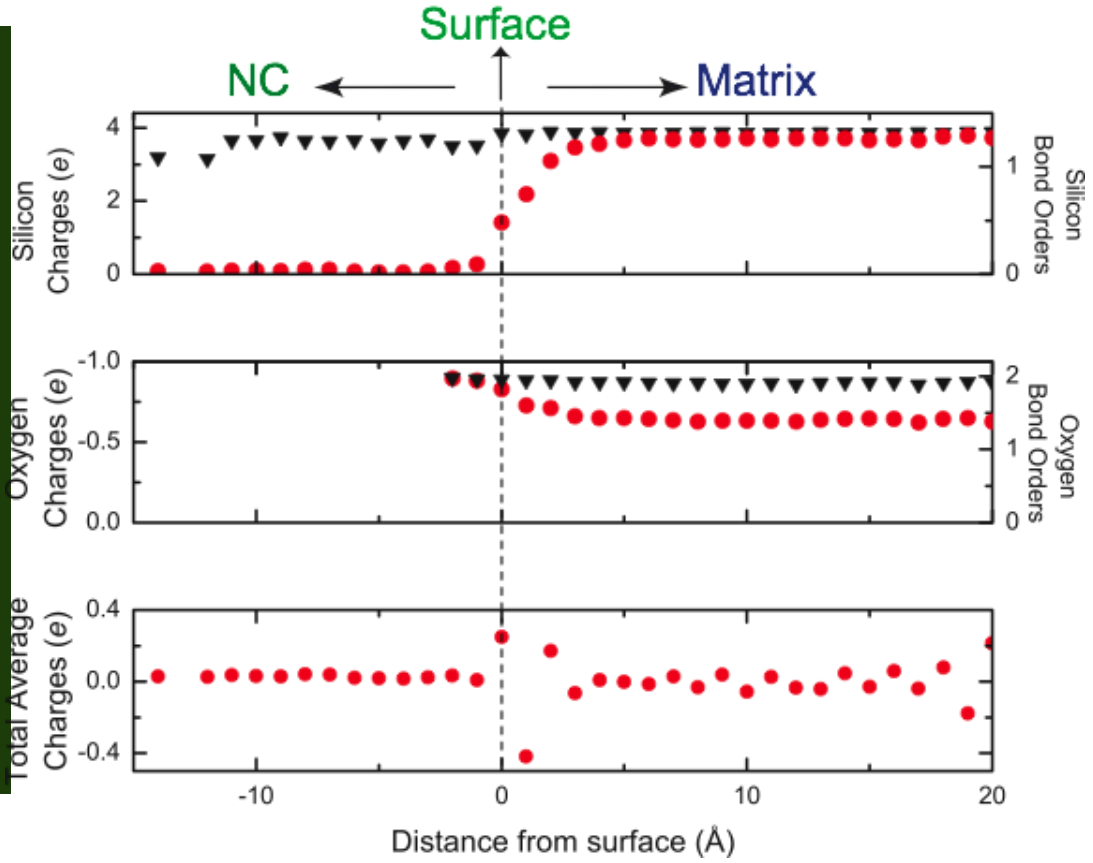

D. Yilmaz, C. Bulutay, T. Cagin, Phys. Rev B 77, 155306 (2008)
D. Yilmaz, C. Bulutay, T. Cagin, Appl. Phys. Lett., (2009) in press

Strain Profile in Si Nanocrystals

- Core of the NC is unstrained.
- Volumetric strain and hydrostatic strain (calculated with Pryor's method) shows similar behavior as expected.
- Bond lengths and strain shows opposite behavior.

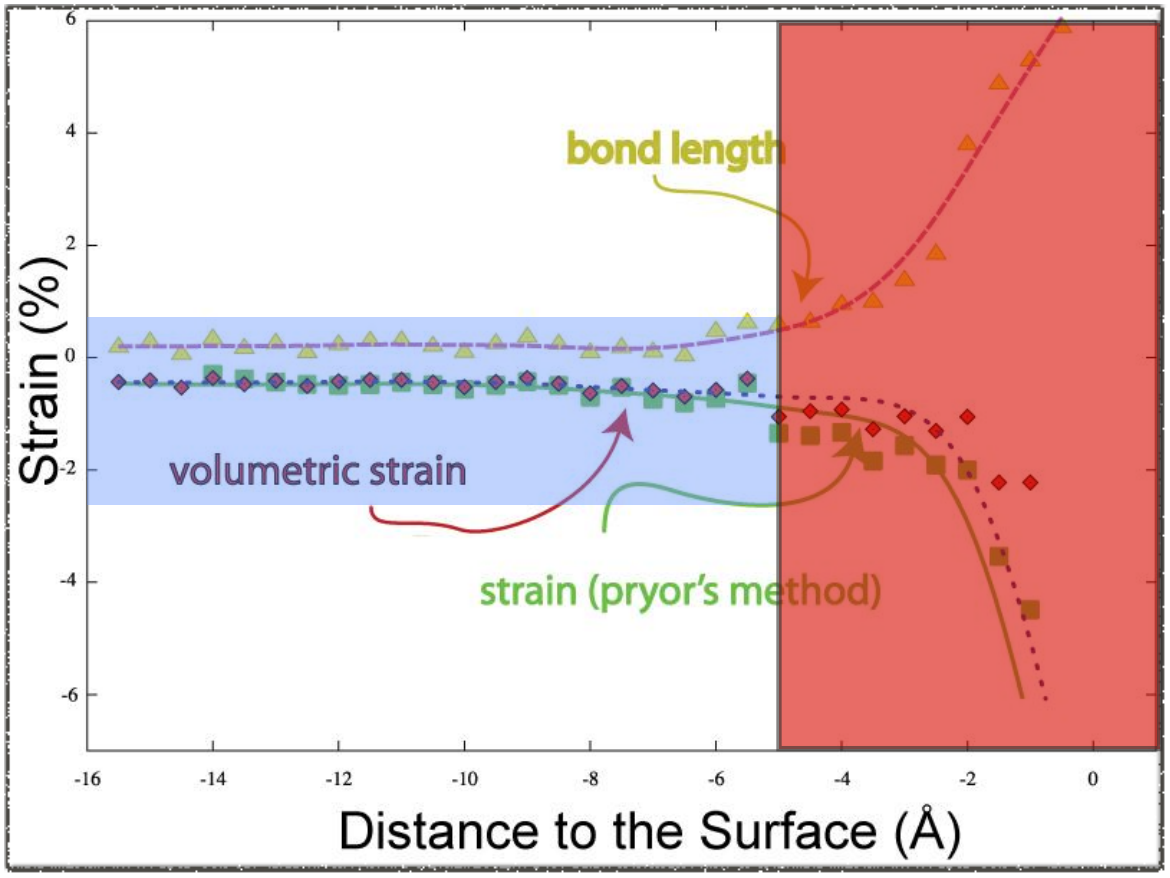

TNT-AFP complexation

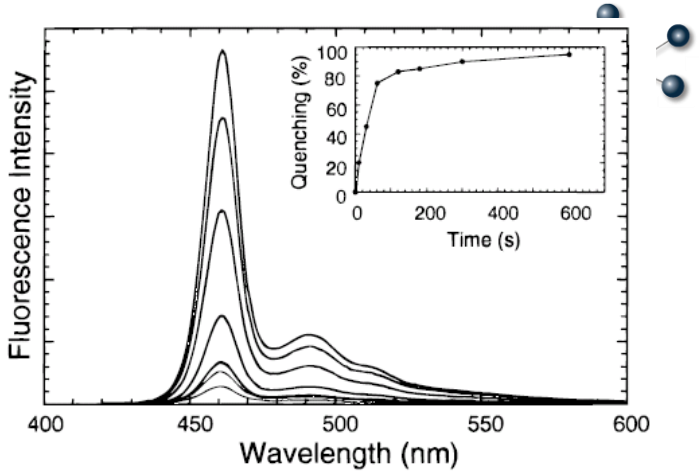

Amplifying Fluorescent Polymer

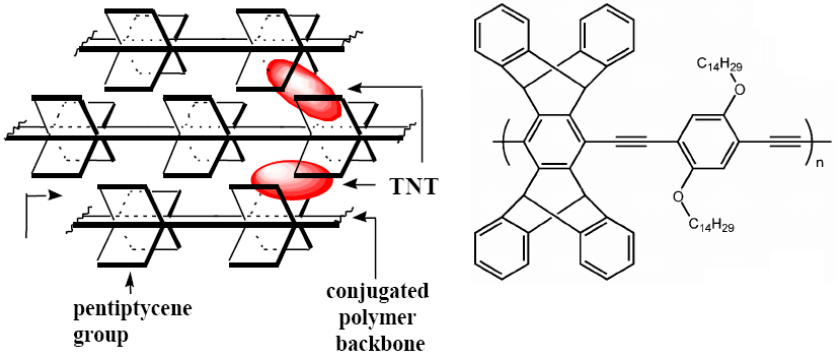

10^{-15} g detection limits (Fido™, Nomadics Inc.)

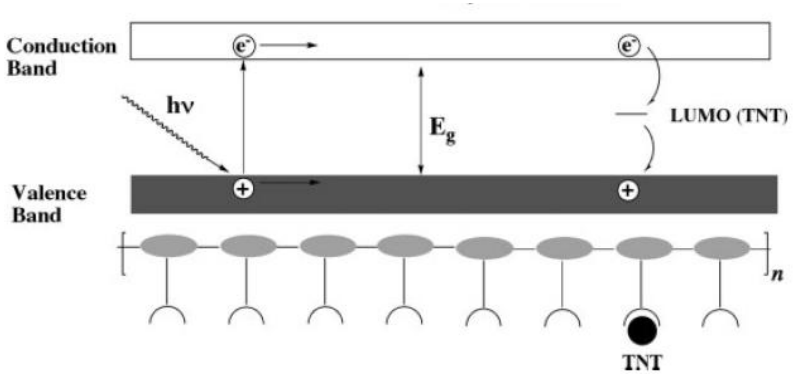

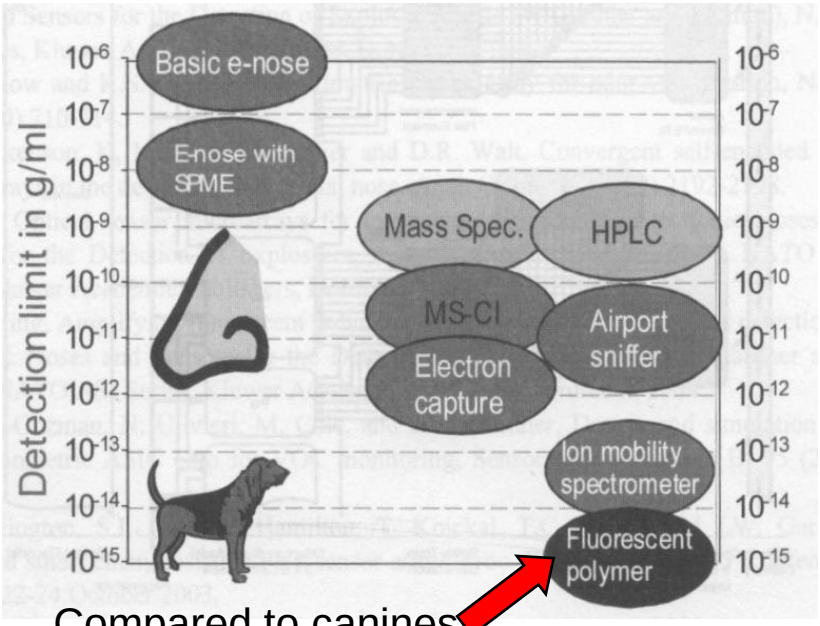

Compared to canines

Yang, J.S. and T.M. Swager,JACS 120, 1998.

B. Arman, H. Fan, T. Cagin, **Quantum Chemical Study of Sensing Mechanism of Nitroaromatics by Amplified Fluorescent Quenching Polymers** J. Chem. Phys. submitted.

Molecular Wire Concept

AFP

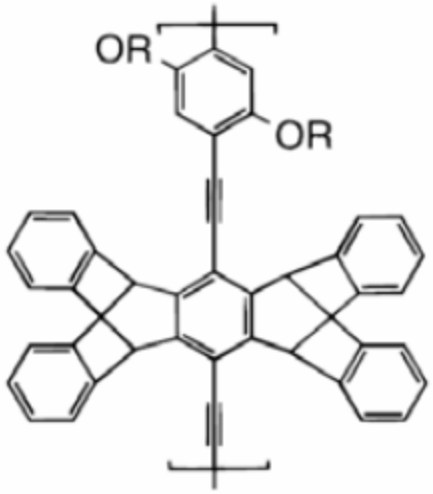

(R = $C_{14}H_{29}$)

I)

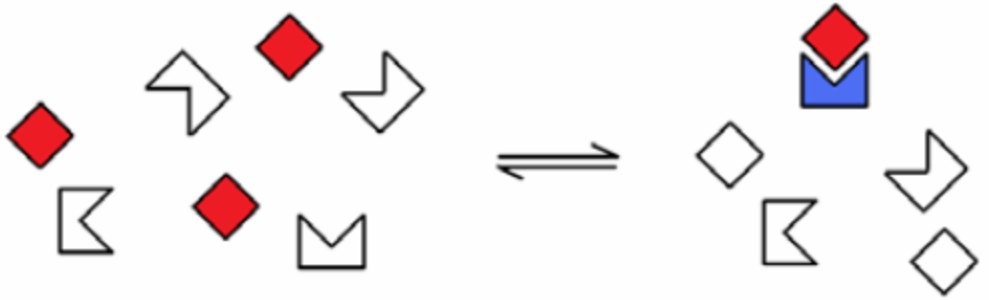

II)

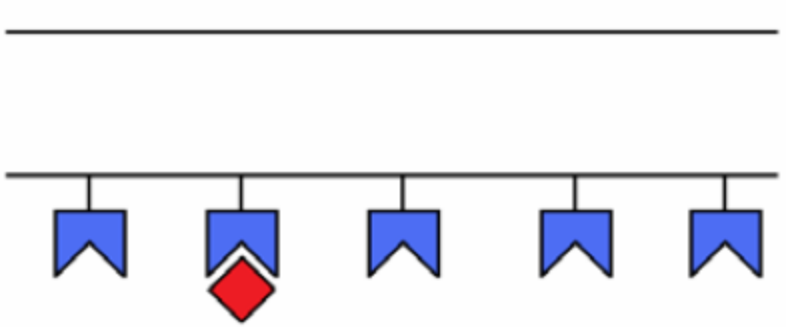

Analyte (TNT)

Receptor

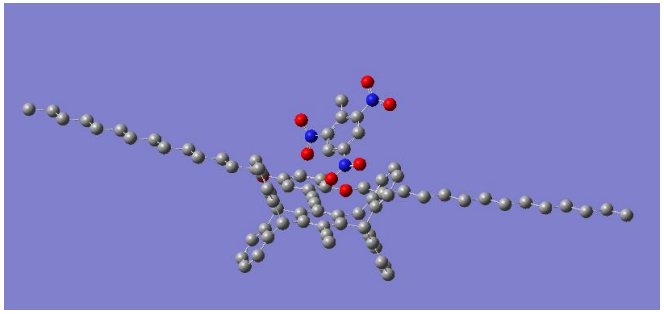

Quenching

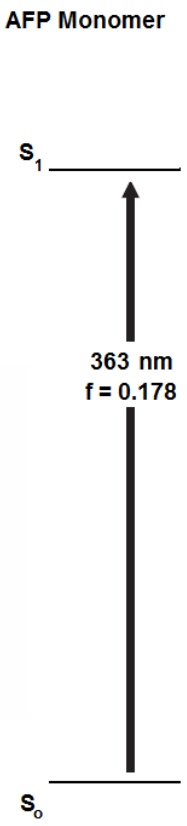
AFP Monomer
S1
363 nm
f = 0.178
So

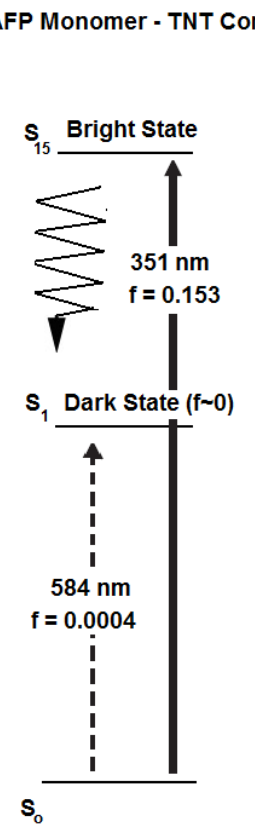
AFP Monomer - TNT Complex
S15 Bright State
351 nm
f = 0.153
S1 Dark State (f~0)
584 nm
f = 0.0004
So

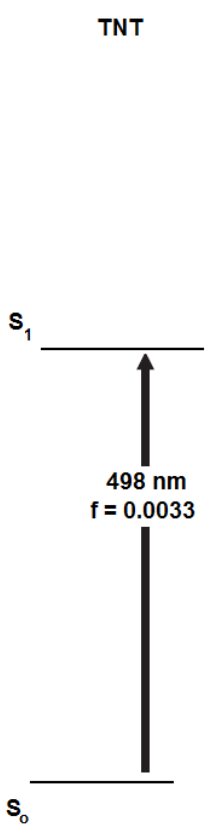
TNT
S1
498 nm
f = 0.0033
So

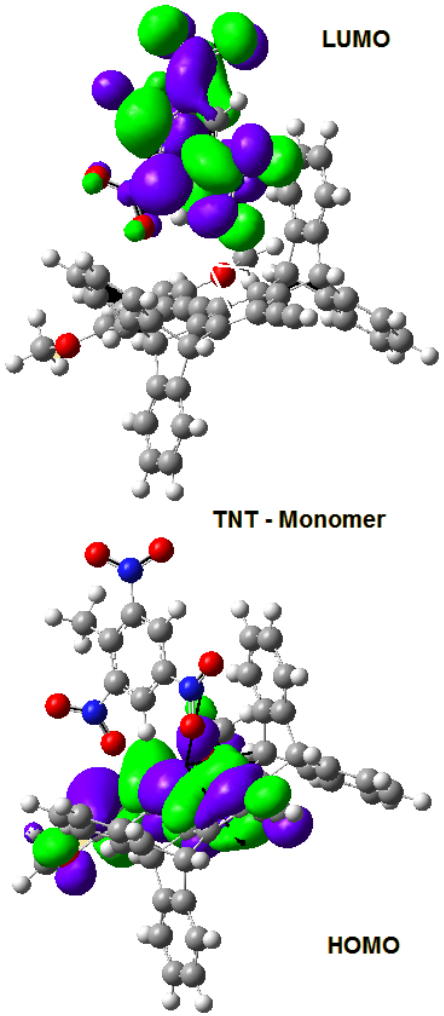
LUMO
TNT - Monomer
HOMO

Time Dependent DFT study of IED Sensing Mechanisms

B. Arman, H. Fan, T. Cagin, J. Chem. Phys. Submitted.

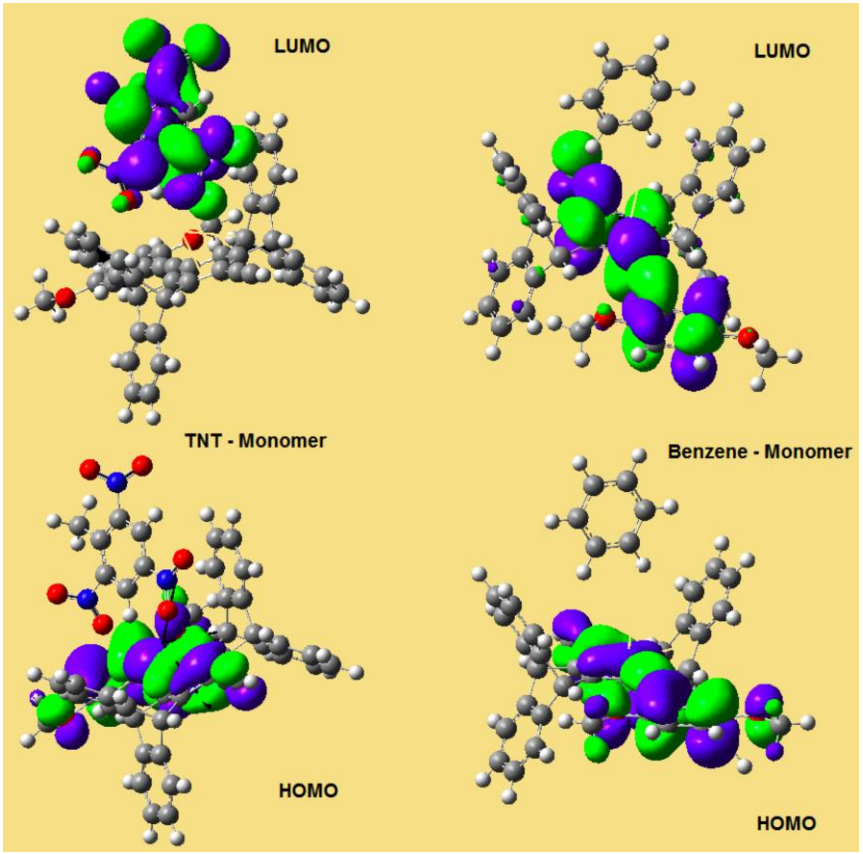

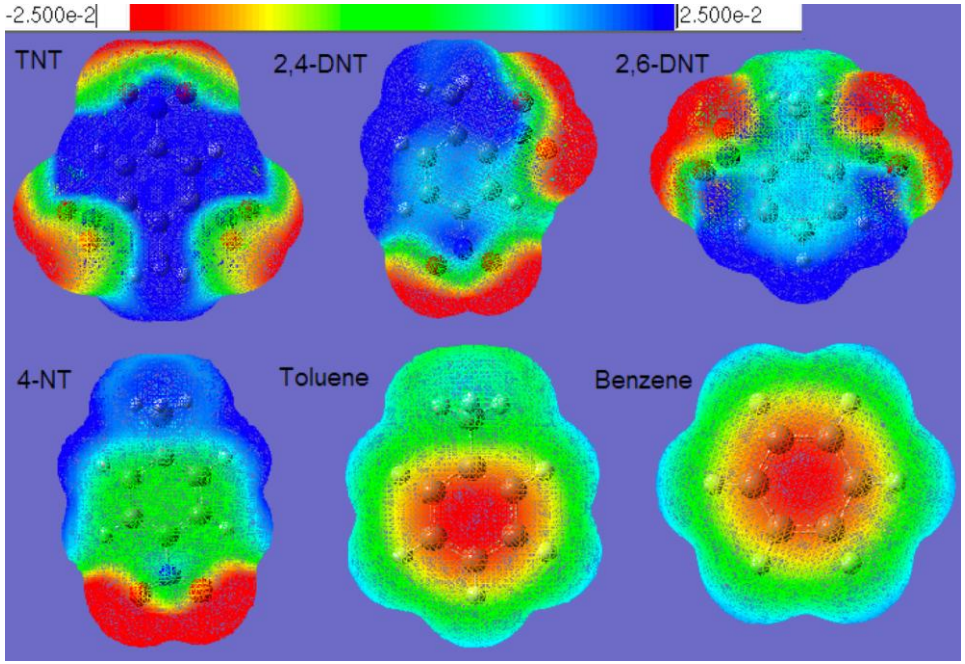

TNT	-3.92990
2,4-DNT	-3.40907
2,6-DNT	-3.28362
4-NT	-2.79245
Toluene	-0.34776
Benzene	-0.39294

Analyte Name	Analyte Homo Lumo-Gap (eV)	Analyte-Monomer Homo-Lumo Gap (eV)
TNT	**4.880**	**2.029**
2,4 DNT	**5.004**	**2.360**
2,6 DNT	**4.948**	**2.390**
4 NT	**4.862**	**2.927**
Toluene	**6.328**	**3.966**
Benzene	**6.602**	**3.967**

Stability and Optimization

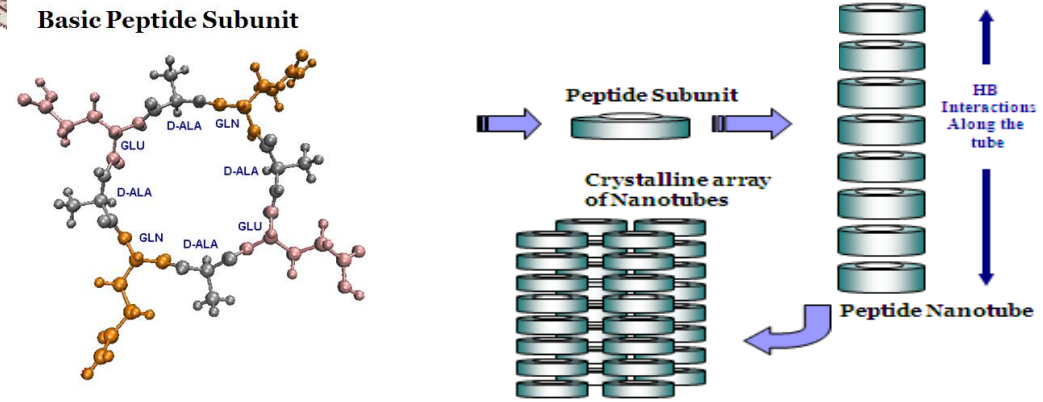

Name	Exp.	Sim.
a	9.5 A	9.6 A
b	15.1 A	15.3 A
c	15.1 A	15.1 A

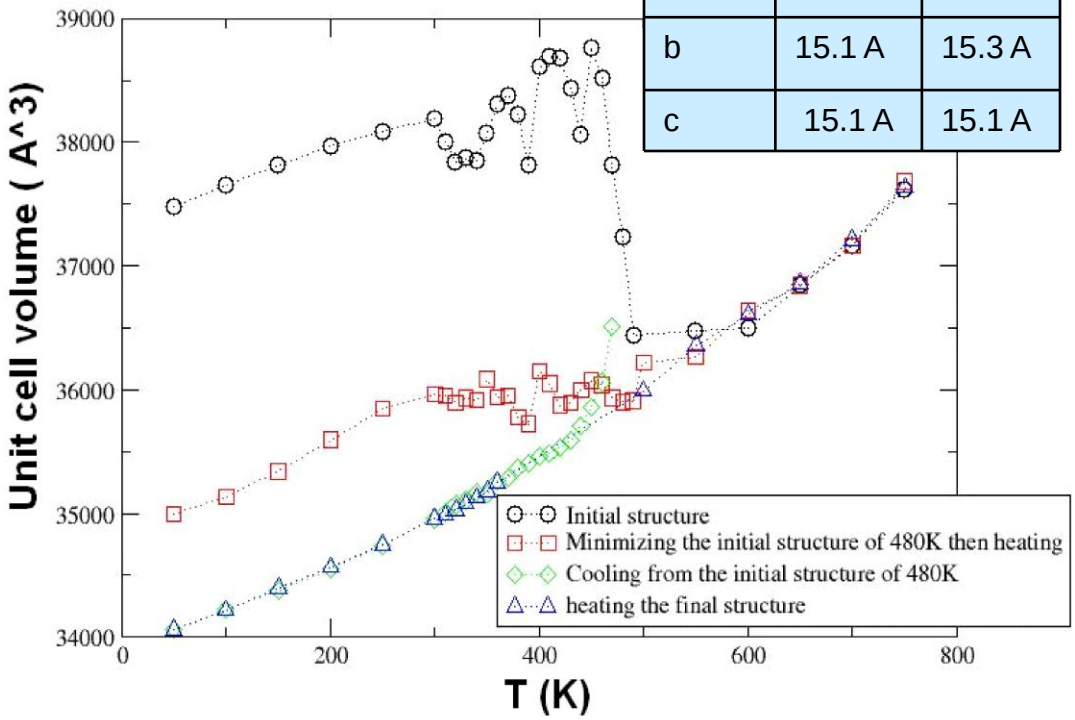

Crystalline nanotubes

8-Peptide System

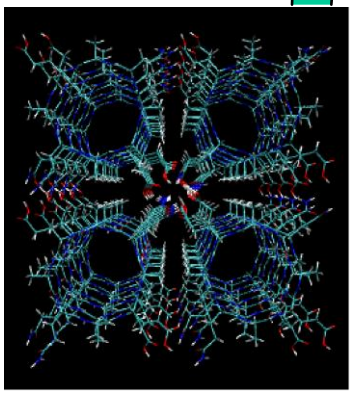

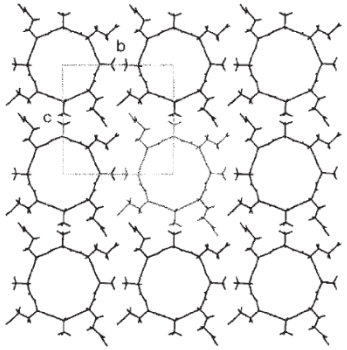

12-Peptide System

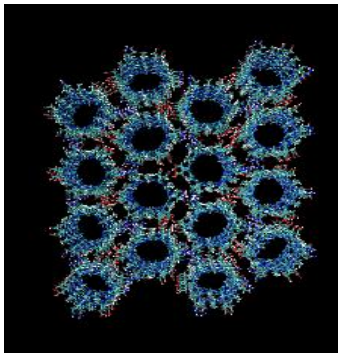

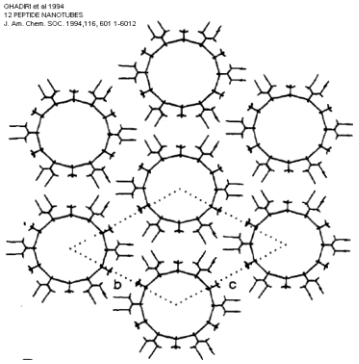

Transport Properties

Diffusion of water in Peptide Nanotubes is faster compared with equivalent diameters of CNTS.

Self Diffusion Coeficient

$$\left\langle (x(t+\Delta t)-x(t))^2 \right\rangle = 6*D*t$$

Einstein's Relationship

DETAILS
From the analysis of curves of mean square displacement along axial direction.

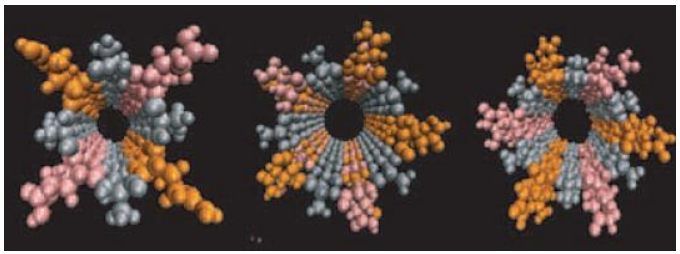

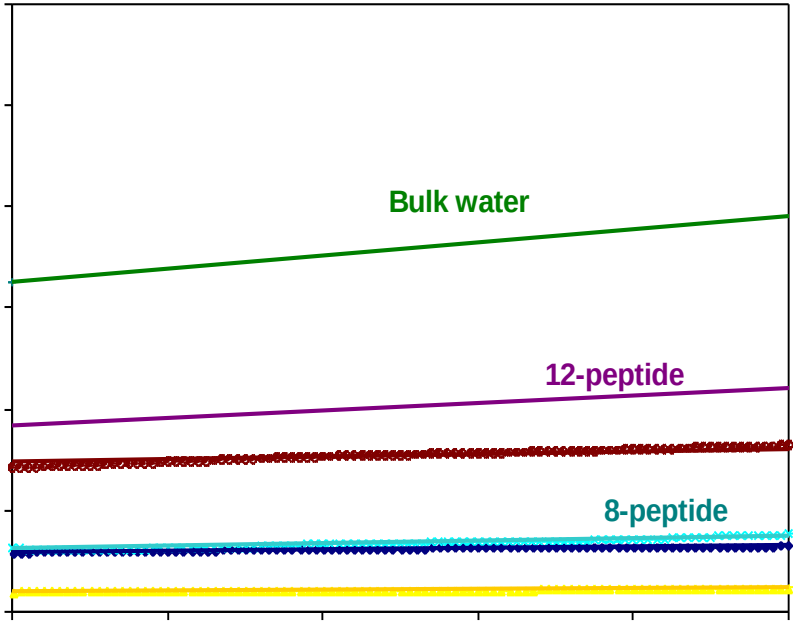

System	Diameter (A)	Diff. coeff. (calc) cm^2/s $(1*10^5)$
Bulk water	—	2.17
12-peptide	14	1.23
(15,15) CNT	15	0.41
8-peptide	8.8	0.41
(9,9) CNT	8.6	0.25
(8,8) CNT	7.2	0.13

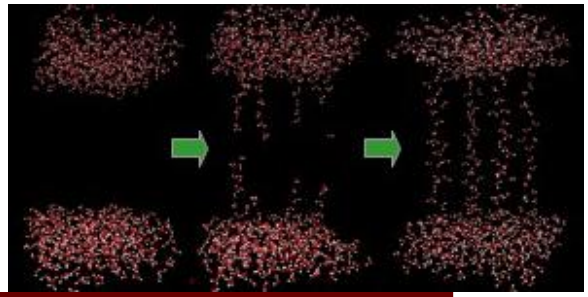

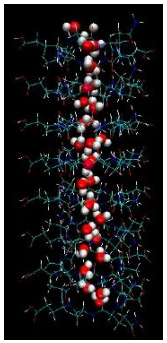

Mechanical Properties

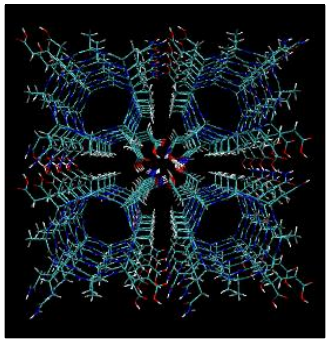

SIDE CHAIN- SIDE CHAIN INTERTUBULAR HYDROPHOBIC INTERACTIONS

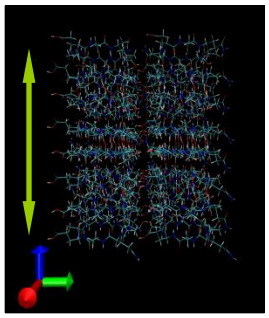

HYDROGEN BONDING INTERACTION ALONG THE NANOTUBES

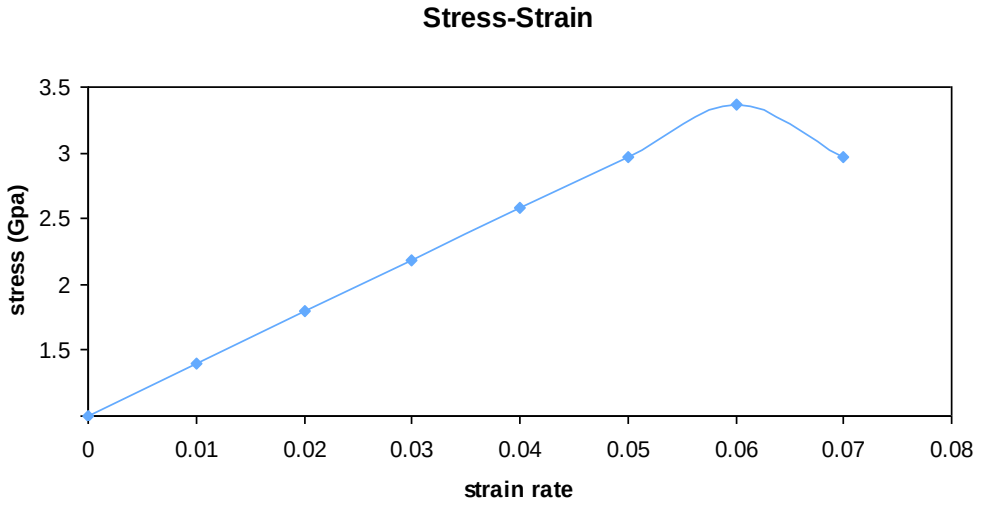

$$\Delta E = \frac{Vo}{2}\sum C_{IJ}\eta_I\eta_J + \frac{Vo}{6}\sum C_{IJK}\eta_I\eta_J\eta_K$$

Anisotropic Isothermal Elastic Constants

Cij	value(Gpa)	Cij	value(Gpa)
C11	8.09	C66	0.77
C22	10.16	C12	6.56
C33	19.65	C13	9.56
C44	1.23	C14	0.57
C55	1.23	C23	9.59

Experimental Young Modulus reported for Peptide Nanotubes :19GPa. *Self-Assembled Peptide Nanotubes Are Uniquely Rigid Bioinspired Supramolecular Structures. Nano Lett., 2005, 5 (7), pp 1343-1346*

Stress-Corrosion Cracking (SCC) in Fe

- Concerns vast range of application
- Combined influence of stress & corrosive environment
- SCC is proved to be connected to GB
  - introduction of impurity element
  - giving no sign of warnings

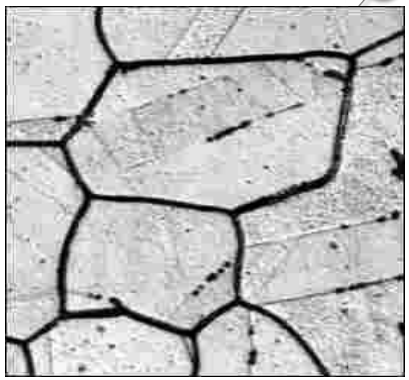

(Source: Corrosion testing lab)

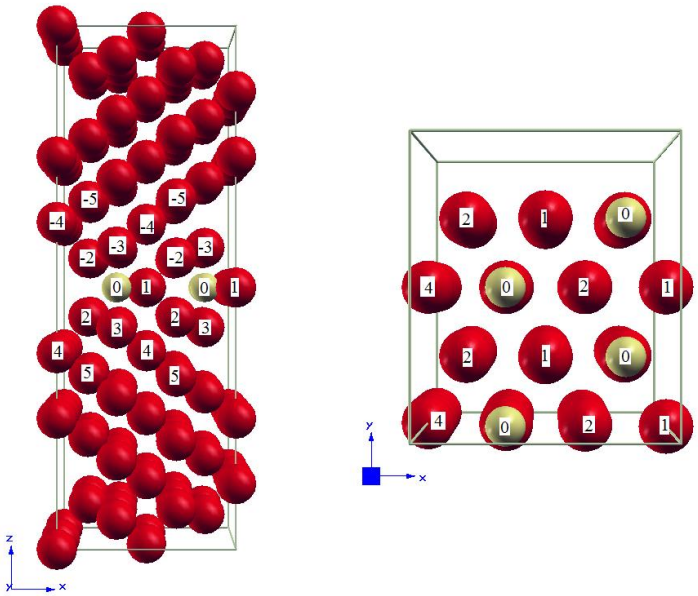

Σ3 (111) grain boundary - 96 Fe atoms

Binding energy

$$E_b N_I = E_{tot}^{GB}(N_{Fe}, N_I) - N_I E_I - E_{tot}^{GB}(N_{Fe}^0) - \frac{N_{Fe} - N_{Fe}^0}{N_{Fe}^0} E_{tot}^{bulk}(N_{Fe}^0)$$

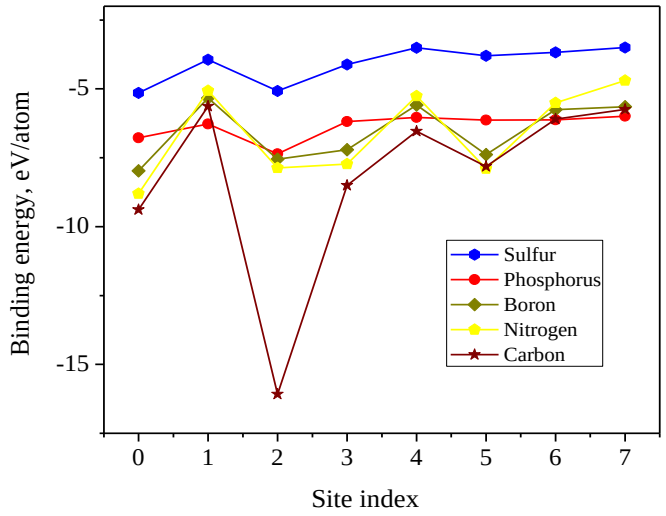

- Carbon ties strongly
- GB0 & GB+/-2 are favorite sites: geometry other than chemistry

Behavior of Sulfur segregation

Fig. Average binding energy of Sulfur as function of layer occupation

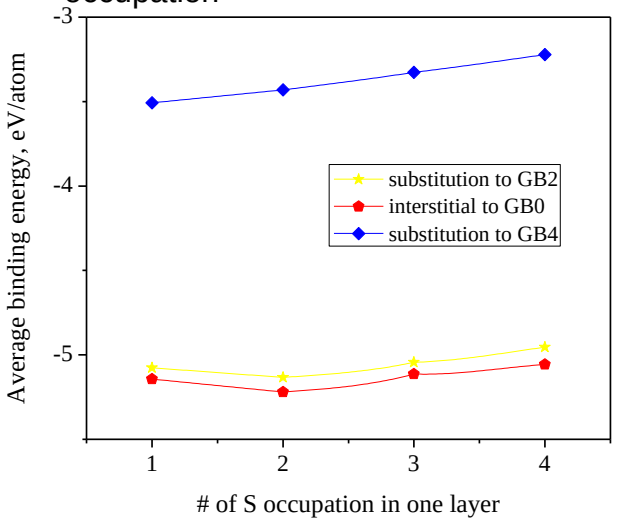

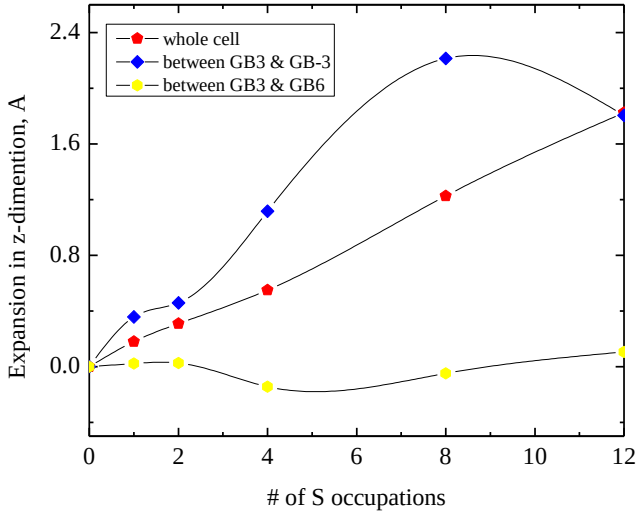

Tab. Behavior of GB cell under S attachment
a, b, c - size of GB cell in x, y, and z dimaentions, respectively
d - distance between GB3 & GB-3

layer	# of occ.	a, Å	b, Å	c, Å	d, Å	- Eb/S, eV
clean cell	0	6.92	7.99	20.29	3.15	--
GB0	1	6.92	8.00	20.47	3.51	-5.14
	2	6.92	8.03	20.60	3.61	-5.22
	3	6.96	8.00	20.75	3.68	-5.11
	4	6.96	8.02	20.84	4.27	-5.06
GB0 & GB2	8	6.89	7.96	22.12	5.36	-4.86
GB0 & GB2 & GB-2	12	6.94	8.02	22.12	4.95	-4.46

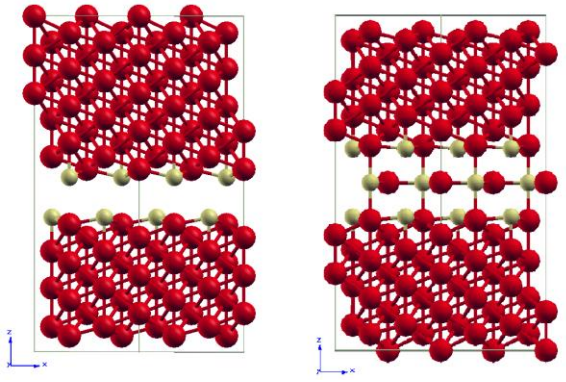

8S 12 S

- z-expansion due to GB separation
- S atoms expose repulsive forces
- interactions around GB broken

Behavior of GB cell under P, N, C and B attachment

Elements	# of occ.	Δa, Å	Δb, Å	Δc, Å	Δd, Å	- Eb/S, eV
P	1	0.00	0.00	0.19	0.34	-6.78
	2	0.00	0.00	0.37	0.45	-7.46
	4	0.01	0.02	0.60	1.15	-7.41
	8	-0.04	-0.06	0.80	1.14	-6.22
	12	0.10	-0.14	1.13	1.25	-5.91
N	1	0.03	-0.01	-0.02	0.29	-8.80
	2	0.02	0.05	-0.03	0.39	-8.95
	4	0.09	-0.01	0.04	0.41	-7.92
	8	0.16	-0.10	-0.08	0.17	-8.15
	12	0.22	-0.21	-0.30	-0.25	-7.74
C	1	0.02	0.00	-0.01	0.25	-9.38
	2	0.02	0.04	-0.02	0.31	-9.40
	4	-0.02	-0.01	0.21	0.56	-8.85
	8	-0.05	-0.05	0.13	0.39	-7.92
	12	-0.19	-0.23	0.53	0.33	-7.42
B	1	-0.01	-0.01	0.08	0.25	-7.98
	2	-0.01	-0.02	0.18	0.27	-7.96
	4	-0.04	-0.04	0.40	0.81	-7.94
	8	-0.07	-0.10	0.20	0.61	-6.98
	12	-0.16	-0.18	0.50	0.52	-6.39

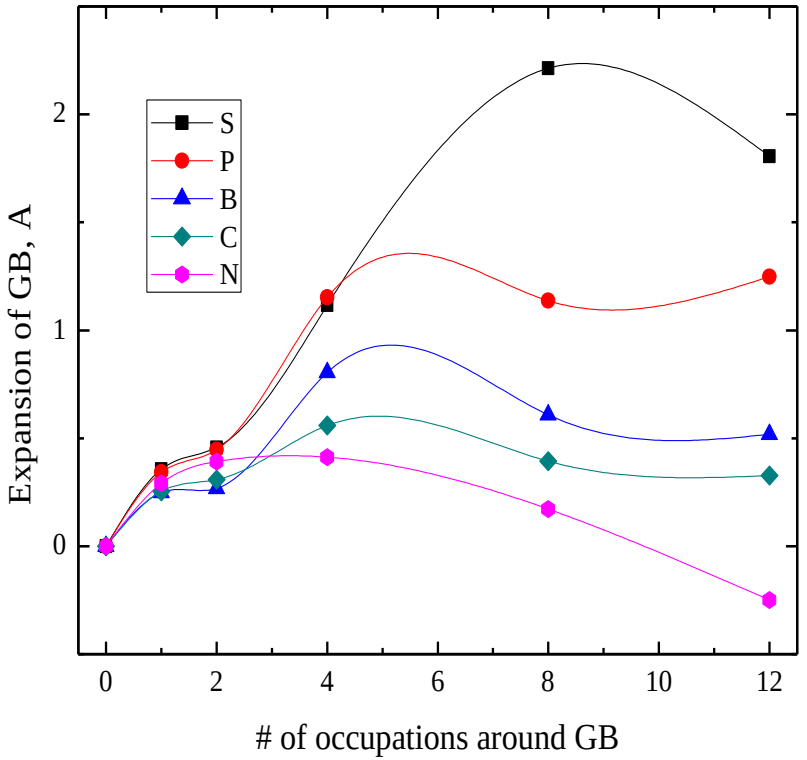

Fig. Comparative separation of Fe Σ3 (111) GB under the attack of different impurity atoms (S, P, N, C, B)

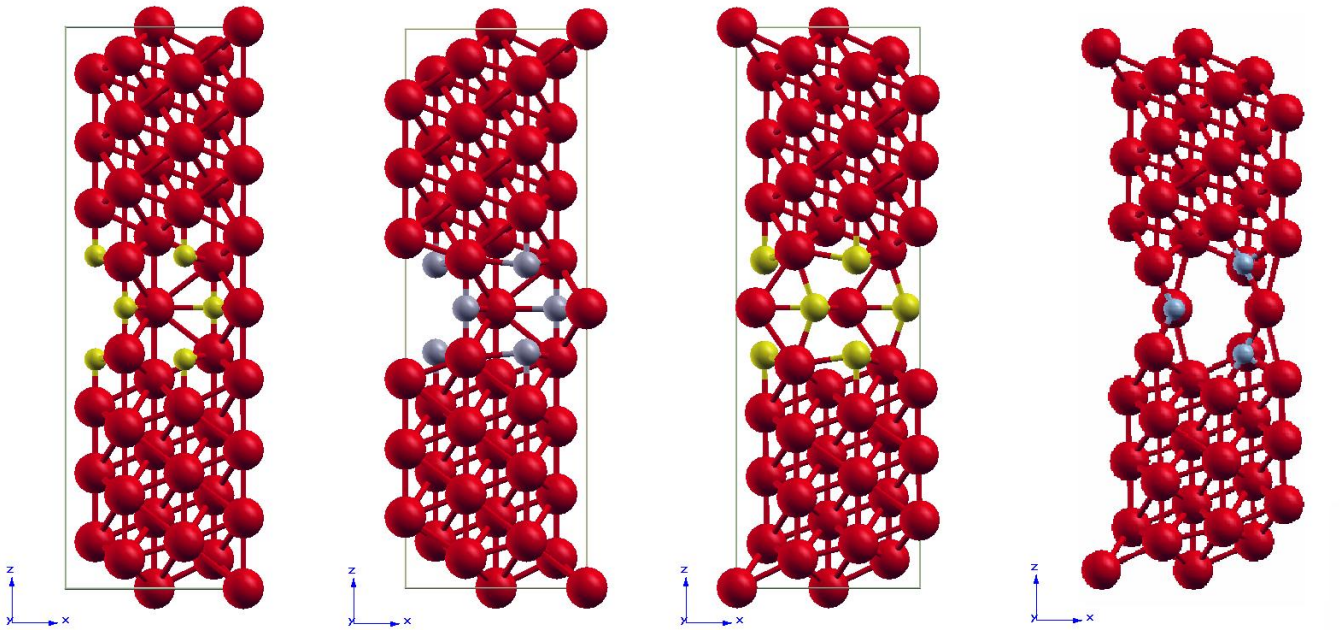

Fig. Behavior of Fe Σ3 (111) GB due to the precipitation of C, B, P and N

- The same binding tendency to a specific locations at GB
- Little interactions from impurity particles on the same layer
- S & P causes the separation of GB, which may initiate cracks
- B & C have little effects on GB mechanical properties
- N weakens the GB structure through formations of cavities and voids

- **First Principles DFT+U studies on (Ce,Th) O2 alloys**
  - Structure, Mechanics, Dynamics, Alloying of CeO2 and ThO2
  - C. Sevik, T. Cagin, "Mechanical and electronic properties of CeO2, ThO2, and (Ce, Th)O2 alloys" submitted to Phys Rev B. (2009)

Calculated lattice parameters, mechanical properties for CexTh1−xO16.

	a0	B0	C11	C12	C44	Alloy
LSDA+U	5.571	214	379	131	104	Ce1Th7O16
LDA	5.507	216	386	131	95	
LSDA+U	5.548	215	382	132	101	Ce2Th6O16
LDA	5.488	215	385	130	92	
LSDA+U	5.500	213	382	129	96	Ce4Th4O16
LDA	5.448	210	379	126	87	
LSDA+U	5.450	215	386	130	88	Ce6Th2O16
LDA	5.405	209	377	125	79	
LSDA+U	5.425	216	388	130	85	Ce7Th1O16
LDA	5.383	208	376	124	76	

High speed particle impact on atomic scale

- Radiation damage, degradation and embitterment (nuclear material shields, space gadgets etc.)
- Ion implantation, deposition (semiconductor device production)
- Surface modification (surface hardening, corrosion resistance etc.)

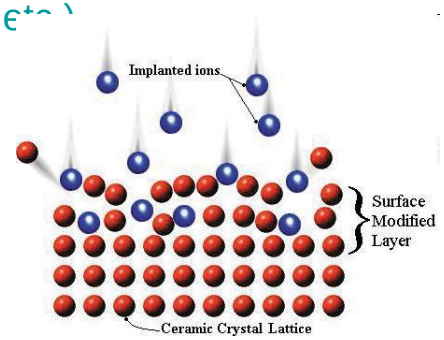

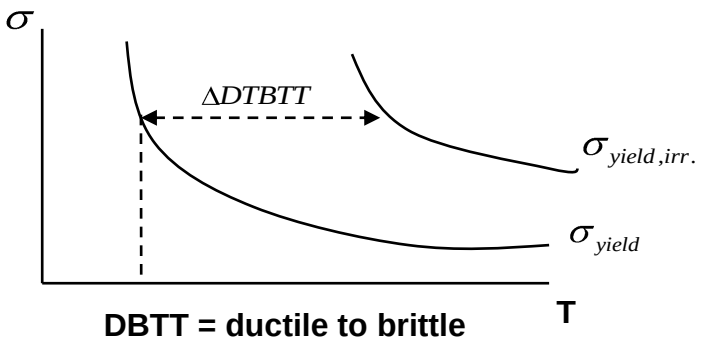

DBTT = ductile to brittle transformation temperature

Molecular Dynamics simulations of irradiation process

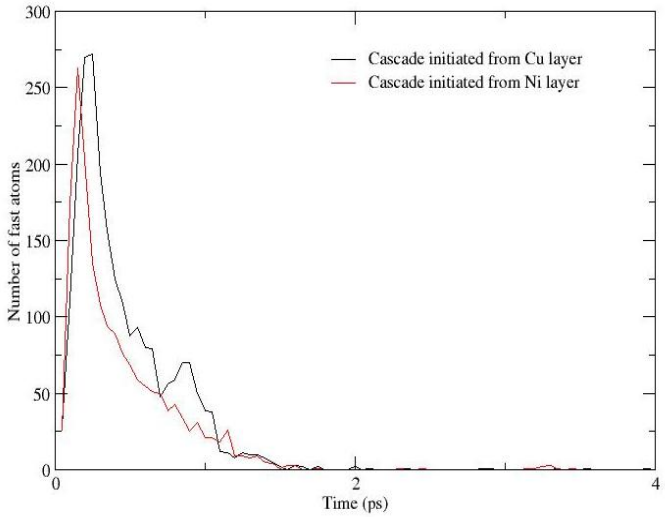

Thermal spike and following thermalization in Cu-Ni superlattice

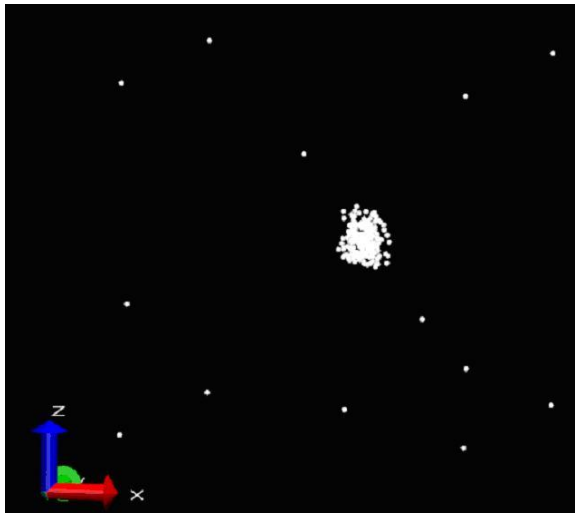

Simulation of microstructure evolution under irradiation in Cu-Ni superlattice

Magnetic Shape Memory Alloys -Ni_2MnIn

- **Heusler alloy** structure
  - L21 in austenite phase
- Ferromagnetic due to separation of magnetic moments residing on Y atoms
- Ni_2MnGa most extensively studied, with reported recoverable strains ≈10% in the martensite phase

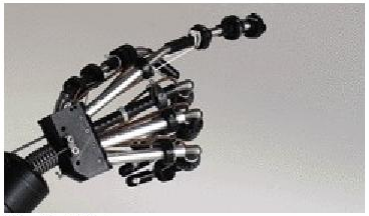

University of Alberta

USAF Aircraft Pictures - http://sun.vmi.edu/hall/afpics.htm

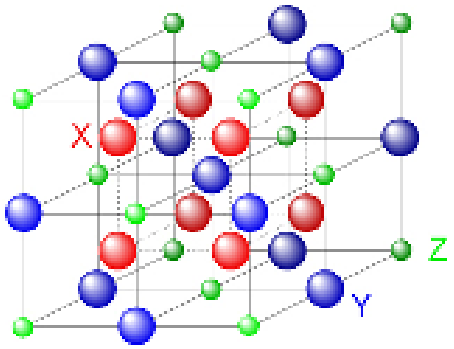

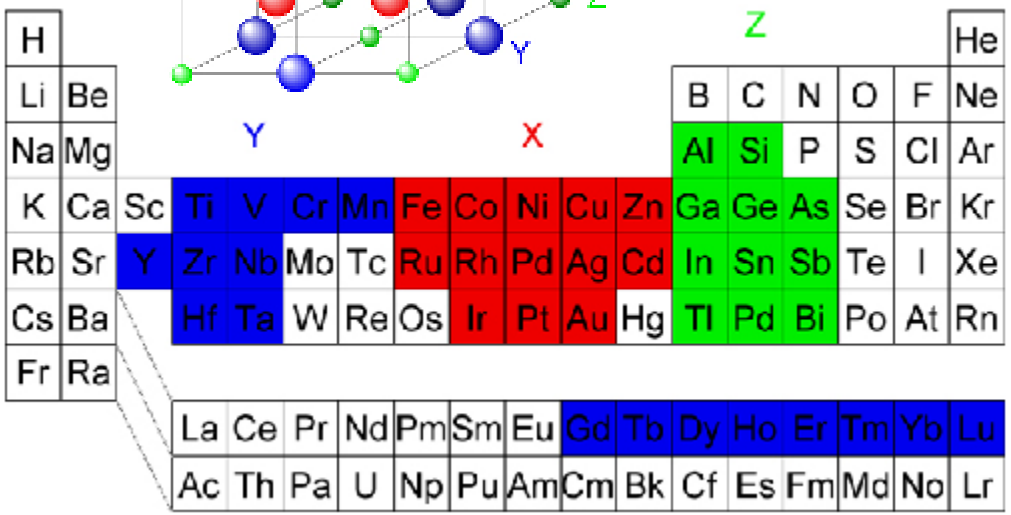

http://www.riken.jp/lab-www/nanomag/research/heusler_e.html

Magnetostructural Coupling in Ni_2MnIn

We apply volume-conserving strains to determine the magneto-mechanical response:

-tetragonal shear

$$\varepsilon = \begin{bmatrix} \delta & 0 & 0 \\ 0 & \delta & 0 \\ 0 & 0 & \dfrac{-\delta^2 - 2\delta}{(\delta+1)^2} \end{bmatrix}$$

-pure shear

$$\varepsilon = \begin{bmatrix} 0 & \delta & 0 \\ \delta & 0 & 0 \\ 0 & 0 & \dfrac{\delta^2}{1-\delta^2} \end{bmatrix}$$

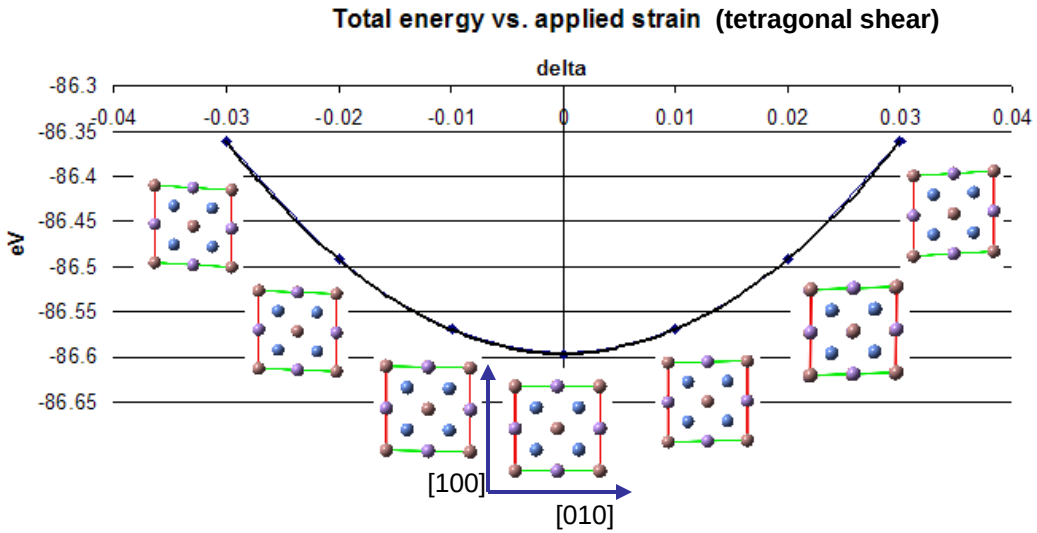

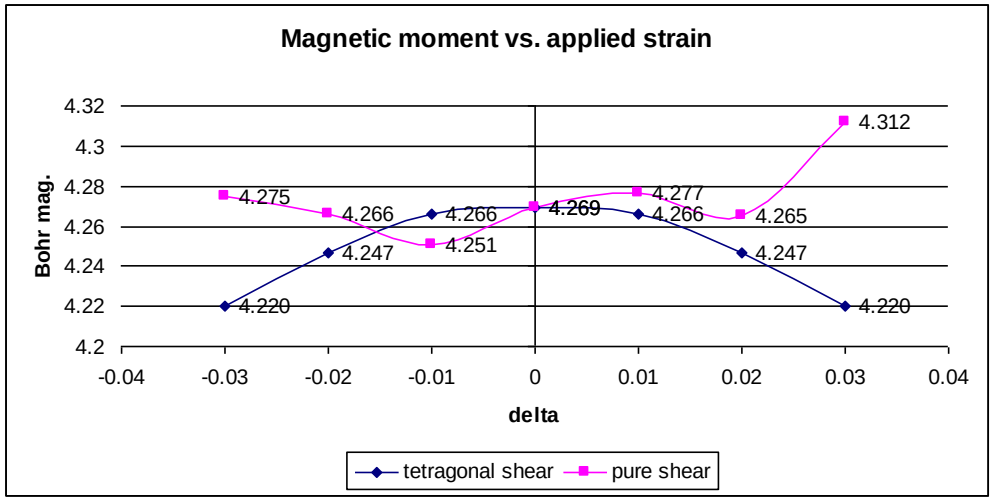

Polyimide-nanotube composites for electro-active materials

A. CHAKRABARTY, T. CAGIN, CMC 3, 167 (2008); MMM (2008)

- (ß – CN)APB/ODPA Polyimide
- Piezoelectric polyimide
- Exceptional thermal, mechanical, and dielectric properties
- Amorphous in nature
- Potential use in high temperature application

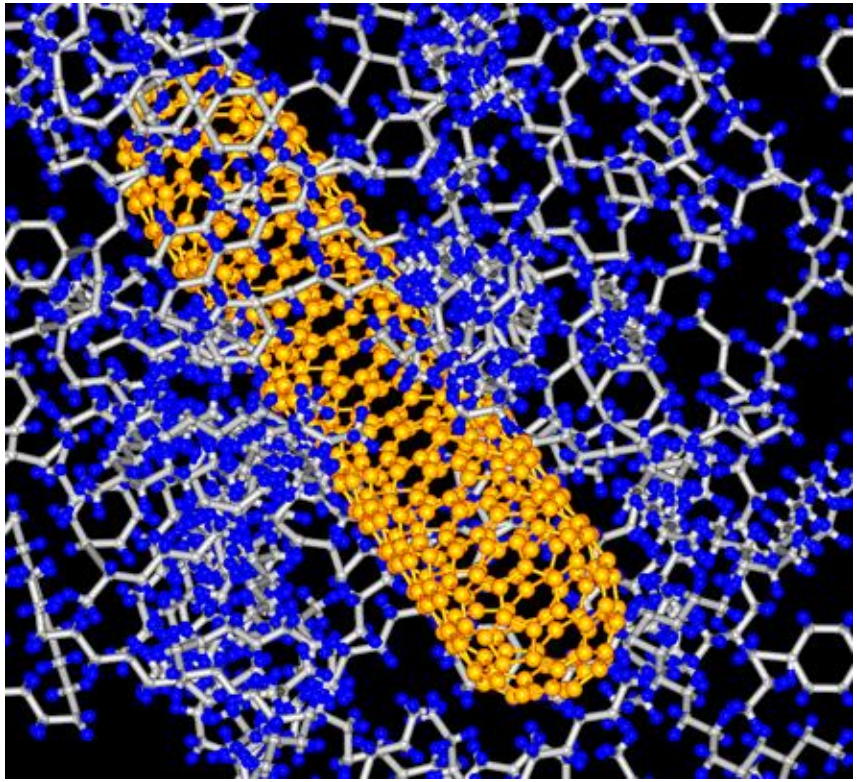

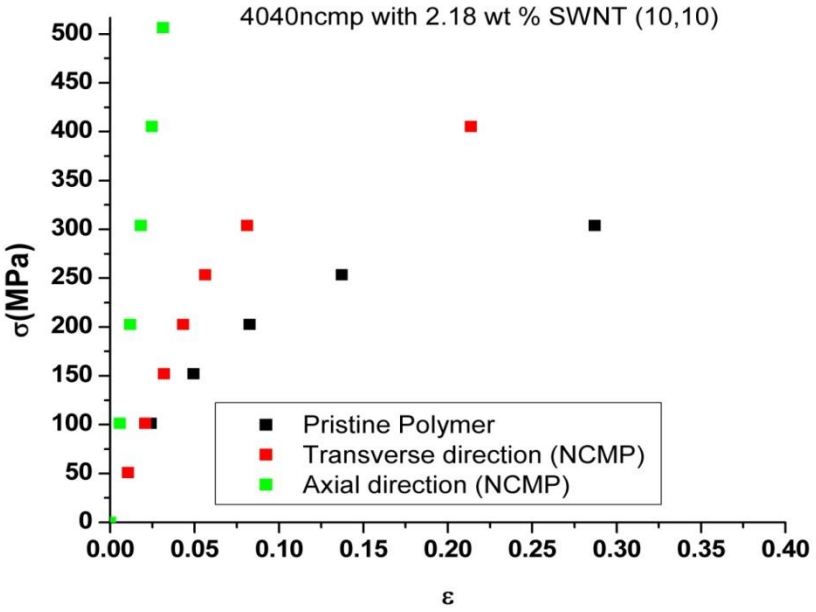
4040ncmp with 2.18 wt % SWNT (10,10)
σ(MPa)
ε
Pristine Polymer
Transverse direction (NCMP)
Axial direction (NCMP)

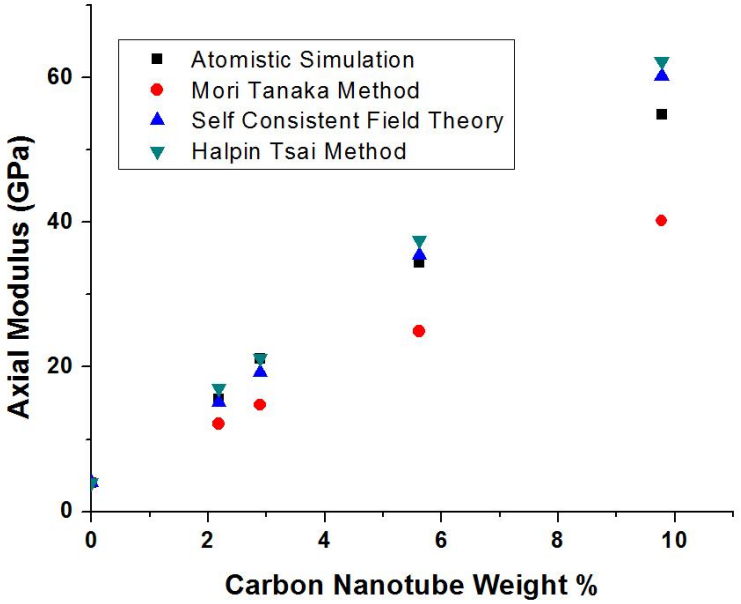
Atomistic Simulation
Mori Tanaka Method
Self Consistent Field Theory
Halpin Tsai Method
Axial Modulus (GPa)
Carbon Nanotube Weight %

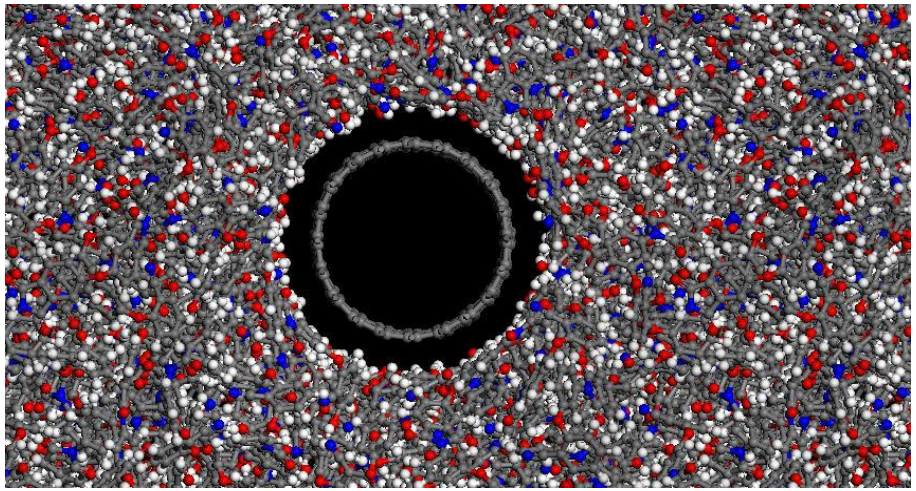

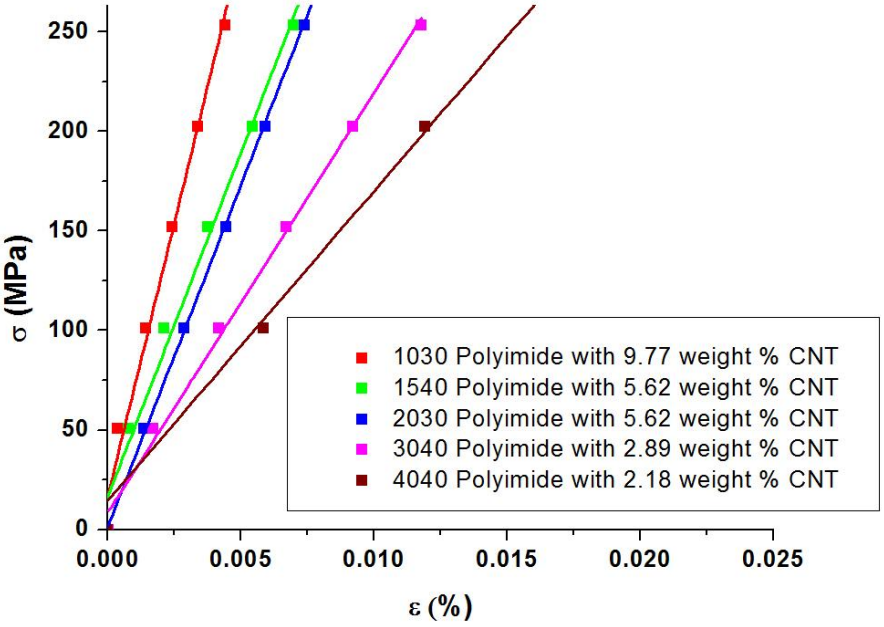
σ (MPa)
ε (%)
1030 Polyimide with 9.77 weight % CNT
1540 Polyimide with 5.62 weight % CNT
2030 Polyimide with 5.62 weight % CNT
3040 Polyimide with 2.89 weight % CNT
4040 Polyimide with 2.18 weight % CNT

Acknowledgements

Financial Support: NSF, DARPA, ONR, ARO, DOE, & AFRL

NSF (ITR-ASE: stress corrosion)
NSF (IGERT): nanofluidics, SMA, CPNTs
NSF: fire retardant PNC's
DARPA (PROM: FE and TE materials)
ONR (Energetic Materials)
ONR (H-Pd under extreme conditions)
ARO (Energetic Materials)
AFRL (Thermo electrics)
AFRL (IED Sensing)
DOE (Nuclear Fuels)
DOE (Multiscale Modeling)
CONACyT (Domain walls in FE devices)
CONACyT (Dielectric Gate Stacks)
TAMU (Transport in bio-nano systems)
PIIF (H-storage systems)
TUBITAK (Si-nanocrystals)
TUBITAK (MSMA's)
PMMA thin film electronics

TAMU Super Computing Facility

ARMAN, HASKINS
CHAKRABARTY, KINACI, SEVIK
PHAM, SHIV, OJEDA, CAGIN
KAMANI, LIZAROZU
BISWAS, CARVAJAL, WILLIAMS, NJOREGE